

Published in final edited form as:

Nature. 2022 July 27; 608(7922): 336–345. doi:10.1038/s41586-022-05010-7.

Dairying, diseases and the evolution of lactase persistence in Europe

A full list of authors and affiliations appears at the end of the article.

Abstract

In European and many African, Middle Eastern and Southern Asian populations lactase persistence (LP) is the most strongly selected monogenic trait to have evolved over the last 10,000 years¹. While LP selection and prehistoric milk consumption must be linked, considerable uncertainty remains concerning their spatiotemporal configuration and specific interactions^{2,3}. We provide detailed distributions of milk exploitation across Europe over the last 9k years using c. 7,000 pottery fat residues from >550 archaeological sites. European milk use was widespread from the Neolithic period onwards but varied spatially and temporally in intensity. Surprisingly, comparison of model likelihoods indicates that LP selection varying with levels of prehistoric milk exploitation provides no better explanation of LP allele frequency trajectories than uniform selection since the Neolithic. In the UK Biobank^{4,5} cohort of ~500K contemporary Europeans, LP genotype was only weakly associated with milk consumption and did not show consistent associations with improved fitness or health indicators. This suggests other hypotheses on the beneficial effects of LP should be considered for its rapid frequency increase. We propose that lactase non-persistent individuals consumed milk when it became available, but that under particular conditions and microbiological milieux this was disadvantageous, driving LP selection in prehistoric Europe. Comparison of model likelihoods indicates that population fluctuations, settlement density and wild animal exploitation – proxies for these drivers – provide better explanations of LP selection than the extent of milk exploitation. These findings offer new perspectives on prehistoric milk exploitation and LP evolution.

When our ancestors started to consume the milk of domesticated ruminant animals they set in motion a sequence of events leading to the evolution of lactase persistence (LP)⁶ and ultimately the modern globalised dairy industry, using c.1.5 billion cattle⁷ as the principal milk source. Evidence for prehistoric milk exploitation, based on combined faunal and organic residue analysis, indicates considerable spatial variability. Analysis of sheep/goat

Correspondence to: Richard P. Evershed; George Davey-Smith; Mélanie Roffet-Salque; Mark G. Thomas.

Corresponding author requests to RPE, MR-S, MGT and GD-S.

Author Contribution

RPE, MGT and GDS conceived the overall study. MR-S and RPE generated novel lipid residue data. MR-S., AT, YD and MSL, acquired data, assembled new databases and undertook statistical modelling. GDS and MSL performed the UK BioBank analyses. YD, AT and MGT conceptualised the selection model likelihood analysis. YD and AT performed the selection model testing. AT devised the kernel interpolation and generated Figs 1, 2 and 3. MGT, RPE, GDS, MR-S, YD, AT and MSL wrote the paper. All other authors contributed either critical archaeological information, pottery from excavations, data of various types and expert knowledge. All authors read and approved the manuscript.

Competing interest declaration

The authors have no competing interests.

age-at-death profiles suggest dairy management was concurrent with the domestication of caprines in south west Asia in the 9th millennium BCE^{8,9}. The earliest organic residue-based evidence of dairying locates to 7th millennium BCE northwest Anatolia, and is associated with high proportions of cattle bones in faunal assemblages². It is clear that dairy husbandry and processing technology were brought by the first farmers into Europe via the Mediterranean coast³ and through the Balkans^{10,11} into central Europe^{12–15}, although milk use remains undetected in Neolithic sites of Northern Greece¹⁶. In northern Europe extensive studies of organic residues in pottery and dental calculus show unequivocally that the 4th millennium BCE Neolithic inhabitants of the British Isles and Ireland were accomplished dairy farmers (e.g. refs ^{17–20}). In prehistoric Denmark, there is evidence of milk use alongside aquatic resource processing from 4,000 BCE²¹. In prehistoric Finland, the region of highest milk consumption globally today⁷, milk use appears with the arrival of Corded Ware pottery in the early 3rd millennium BCE, although climate fluctuations may subsequently have triggered returns to hunter-gatherer-fisher subsistence strategies^{22,23}.

Ancient DNA data indicate that most, if not all Early Neolithic people were lactase non-persistent (LNP), and that LP only reached appreciable frequencies in the Bronze and Iron Ages^{24–29}. Such an allele frequency trajectory indicates strong selection favouring LP, and is consistent with selection starting in the Early Neolithic^{29,30}. The main Eurasian LP-causing allele (rs4988235-A; also known as 13,910*T; ref. ³¹) has a highly structured geographic distribution in modern Europe³². This may reflect different strengths of selection in different regions^{33,34}, although other explanations remain similarly plausible, such as modern frequencies being shaped by demographic processes^{30,35} – including an hypothesised Bronze Age Steppe origin²⁶ (but see ref. ²⁹) – or allele distribution reflecting its origin location^{30,36}. A range of hypotheses to explain positive LP selection have been proposed ^{6,25,37–41}. Among these, the *calcium assimilation hypothesis*³³ – whereby milk supplements low vitamin D diets in low incident UVB regions, such as occur in northern Europe, is probably the most widely cited^{42,43}. However, this hypothesis does not explain the inferred high selection strengths in lower latitude regions, such as Africa, the Middle East, Southern Europe and Southern Asia⁴¹, where milk as a source of relatively pathogen-free fluid provides a more plausible explanation³⁷. Cubas et al.³⁴ recently noted a latitudinal cline in the proportion of milk fats in pots in Early Neolithic Atlantic Europe, and argued that as a marker of milk usage this cline explains the modern LP distribution in the same region. Regardless of the proximal and probably regionally-specific drivers of selection on LP, milk consumption is a prerequisite⁴⁴. However, LP is not accompanied at an individual level by meaningful differences in milk consumption^{32,38,45,46} or the risks from a range of diseases⁴⁷ in modern populations, and thus its selection may underpin potential adverse consequences of milk consumption in LNP individuals in certain historically-contingent environments³⁸.

In order to build a more comprehensive picture of prehistoric milk use, and examine how well it explains selection on LP, we compiled all published instances of the occurrence of milk fat residues detected in pottery containers from 366 archaeological sites in Europe and southwest Asia. To improve spatiotemporal coverage we added newly generated organic residues data from 188 sites from various regions and periods. Overall, we utilised 6,899 animal fat residues derived from 13,181 potsherds from 826 phases from 554 sites, with associated georeferences and phase chronology including >1,000 radiocarbon dates. These

data were used to generate time series depicting the frequency of milk use across prehistoric continental Europe from 7 kyr BCE to 1.5 kyr CE (Figure 1), and regional time series (Figures 2 and ED1). The high density of organic residues c.5.5 to 5 kyr BCE in Figure 1b reflects our new sampling; targeted to explore the co-evolution of dairying and LP amongst the first farmers in the central European Linearbandkeramik (LBK) culture³⁰. If we consider the profusion of ^{13}C values -3.1‰ (a proxy for milk fat residues^{17,48,49}, see Methods; Figure 1b), it becomes immediately clear that milk use was a very widespread activity across all periods in European prehistory, and at the broadest scale this was congruous with the spread of farming across the continent.

The extensive sampling and analysis of pottery has enabled us to resolve the spatiotemporal patterning of milk use in unprecedented detail (Figure 2). Importantly, this shows that milk exploitation arrived with the first farmers into the Mediterranean basin (except the region covered by modern day Greece) and continued throughout the Neolithic, whilst the later arrival of the Neolithic in Southern Britain was associated with immediate and high milk use – probably reflecting the arrival of advanced dairying populations from adjacent regions of continental Europe²⁸ – which then gradually reduced. The prehistoric Balkans was the core region for the early intensification of milk use, which is consistent with the rise of cattle exploitation there⁵⁰, yet surprisingly milk use appears largely absent from geographically adjacent Neolithic site phases located in Greece (based on analyses of >190 animal fats from >870 potsherds; however, we note that other types of containers may have been used for milk processing in this cultural context). In some regions our data suggest continuous intensive milk use, notably in western France, northern Europe and the British Isles from 5.5 kyr BCE to 1.5 kyr CE. Despite intensive sampling from central Europe (>2,800 animal fats from >6,810 potsherds), a region previously inferred to be the origin of selection on LP³⁰, the frequency of milk use was consistently lower than for the south east, west or north of Europe throughout prehistory. The overarching picture is that, whilst dairying persisted throughout the Neolithic, its intensity fluctuated substantially in space and through time, suggesting regionally-specific instabilities in food production and cultural changes in dietary preferences. This is consistent with previous studies showing regional ‘boom and bust’ fluctuations in population density across Europe over the same period⁵¹.

LP allele (rs4988235-A) frequency trajectory estimates (Figure 3) based on published ancient DNA data from 1786 prehistoric European and Asian individuals (see subsection Data in the Ancient DNA Analyses section of the Methods), are well-described by a sigmoidal curve, as expected for a selective sweep. Curves fitted only to aDNA broadly predict modern allele frequencies³². We note that while the allele only reaches appreciable frequencies by c.2 kyr BCE²⁹, nearly three millennia after its first detection (earliest LP individual dated to c.4,700-4,600 BCE), the dates of origin, the start of selection, the earliest observation and the reaching of appreciable frequencies of this allele are all distinct ‘events’, each possibly separated by thousands of years²⁹. To examine if milk usage patterns can explain these allele frequency trajectories, we devised a maximum likelihood modelling approach (see Methods), whereby LP selection intensity was determined by the proportion of potsherds with dairy fat residues (as a proxy for milk use). Using simulations, we made sure that our approach had the power to detect an association if there was one, even in the presence of moderate levels of noise in our milk use patterns (see subsection Power analysis

in aDNA Methods). We found that patterns of milk usage provided no better explanation (i.e. no increased probability of observed allele frequency data) than assuming uniform selection in space and through time, *contra* to the claims of Cubas et al.³⁴. As an additional sensitivity test of this methodology, we tried using incident solar radiation as the main environmental variable driving LP selection intensity – in line with the *calcium assimilation hypothesis*³³ – and obtained higher probabilities of the observed allele frequency data (Figures ED2 and ED3A, Table ED1).

Our analysis of potsherd lipid residue and ancient LP allele data suggest that intensity of milk usage – beyond its mere presence – did not drive selection on LP. To explore other explanations for LP selection we first turned to contemporary data. The UK BioBank^{4,5} includes genotypic and phenotypic data from c.500,000 people aged between 37-73 years, recruited between 2006-2010 (<http://biobank.ndph.ox.ac.uk/showcase>). In a subset of approximately 337,000 unrelated participants who classified themselves as “white, British” and have similar genetic ancestry, LP genotypes were out of Hardy-Weinberg equilibrium ($P = 1.46 \times 10^{-18}$; Table ED2) which could reflect genotype-related assortative mating⁵² (for which there is weak evidence for LP; Table ED3), selection into a study, or population structure, amongst other influences⁵³. We found the variant was reliably associated with a 6% increase in odds of consuming fresh cows’ milk compared with soya/no milk (95% Confidence Interval CI 1.04 - 1.09; Figure 4) and a reciprocal 6% decrease in odds of following a lactose-free diet (95% CI 0.87 – 0.99; Figure 4). Only 2.54% of dairy milk consumers were following a lactose-free diet (95% CI 2.37% - 2.71%) suggesting that consumption of lactose-depleted milk was unlikely to introduce strong bias on the genetic association with cows’ milk intake. However, around 92% (95% CI 91.5% - 92.2%) of genetically LNP participants consume fresh cows’ milk (Table 1) and among milk drinkers the LP allele was associated with a small 0.05 SD increase in daily milk servings (95% CI 0.01 – 0.08). Similar results of 0.05 SD increase in total dairy servings/day per LP allele (95% CI 0.04 – 0.07) were obtained from a large meta analysis⁵⁴ of European origin individuals not included in the UK Biobank. This suggests LP has only a small effect on milk consumption, which is at odds with selection hypotheses of nutritional advantages from milk. Consistent with these results, some non-European countries with very low levels of LP have been importing milk in vast quantities in recent years as part of a more general adoption of Western diets.

China, for example, has very low LP frequencies³² and milk was rarely consumed in the early 20th century⁵⁵ but has increased more than 25-fold over the past five decades⁵⁶. These findings bring into question the widely held belief that selection against LNP was the result of detrimental effects of milk consumption in otherwise healthy individuals; notably through inducing stomach cramps, diarrhoea, and flatulence^{41,42,57–59}. One possible explanation for the small effect of LP on milk intake in contemporary data is the use of mealtime lactase supplements which reduce symptoms of lactose intolerance. However, these have only become widely available recently and UK Biobank participants would not have had access to them for most of their life.

We examined phenotypic associations of genetically-predicted LP (Figure 4) to investigate potential pathways through which selection could have occurred. The related calcium

assimilation and vitamin D hypothesis³³ would anticipate LP to be associated with higher vitamin D (-3.33×10^{-3} SD [95% CI -9.22×10^{-3} , 2.56×10^{-3}]) concentration and bone mineral density (3.31×10^{-3} SD [95% CI -5.52×10^{-3} , 0.01]) due to its positive relationship with milk consumption^{54,60,61}. However, these estimates are very close to the null, and the large sample size puts considerable constraints on the magnitude of effects that could exist.

Milk consumption has been hypothesised to increase circulating insulin-like growth factor I⁶² (IGF-1), leading Wiley et al.⁶³ to propose a model of LP selection driven by fitness advantages of IGF-1 acting to increase body size and lower age of sexual maturation. However, there were no meaningful differences in IGF-1 (-2.66×10^{-3} SD [95% CI -8.25×10^{-3} , 2.93×10^{-3}]). Nevertheless, LP allele presence was associated with 0.01 SD (95% CI 0.01, 0.02) higher body mass index (BMI), as previously reported^{54,60,61}, but not with height (6.37×10^{-4} SD [95% CI -3.22×10^{-3} , 4.49×10^{-3}]) consistent with other studies well controlled for population stratification^{64,65}. Whilst statistically robust and replicating what has been observed in other large samples^{54,60,61}, the BMI effect is of small magnitude, and congruent with a small difference in calorie intake consequent of milk consumption.

LP allele association with all-cause mortality (1.00 HR [95% CI 0.97, 1.03]), mother's age of death (-0.01 SD [95% CI -0.01 , -3.03×10^{-5}]) and father's age of death (2.35×10^{-4} SD [95% CI -6.27×10^{-3} , 6.74×10^{-3}]), were all close to the null. These results suggest milk has little or no adverse health effect when consumed by LNP adults in a contemporary population. Another possible driver of selection is the influence of the LP allele on fertility, but we found no meaningful effect of the LP allele presence on number of live births (2.52×10^{-3} SD [95% CI -0.01 , 0.01]) or number of children fathered (5.73×10^{-3} SD [95% CI -2.51×10^{-3} , 0.01]).

Aside from dietary change, a number of other factors are likely to have influenced fecundity and mortality following the establishment of farming communities in Europe, including increased population and settlement density⁶⁶, increased mobility⁶⁷, proximity to animals, frequent crop failure, famine and population collapse⁵¹, and general poor hygiene and sanitation. Most, if not all, of these factors are likely to have increased infectious disease loads, particularly zoonoses (~61% of known and ~75% of emerging human infectious disease today come from animals^{68,69}). Given the widespread prehistoric exploitation of milk shown here (Figure 2), and its relatively benign effects in healthy LNP individuals today, we propose two related mechanisms for the evolution of LP. Firstly, as postulated by Sverrisdóttir et al.²⁵, the detrimental health consequences of high lactose food consumption by LNP individuals would be acutely manifested during famines, leading to high but episodic selection favouring LP. This is because lactose-induced diarrhoea can shift from an inconvenient to a fatal condition in severely malnourished individuals⁷⁰, and high lactose (i.e. unfermented) milk products are more likely to be consumed when other food sources have been exhausted⁷¹. This we name the '*crisis mechanism*', which predicts that LP selection pressures would have been greater during times of subsistence instability. A second mechanism relates to the increased pathogen loads – especially zoonoses – associated with farming and increased population density and mobility⁶⁷. Mortality and morbidity due to pathogen exposure would have been amplified by the otherwise minor health effects of LNP individuals consuming milk – particularly diarrhoea – due to fluid loss and other gut

disturbances, leading to enhanced selection for LP³⁸. We name this ‘*chronic mechanism*’, which predicts that LP selection pressures would have increased with greater pathogen exposure. Crucially, proxies are available for some of the drivers of these hypothesised mechanisms, permitting us to explore the extent to which they explain LP selection, and so allele frequency trajectories, using our maximum likelihood modelling approach. For the ‘*crisis mechanism*’ we use fluctuations in population size (residual fluctuations detrended for overall background growth) as a proxy for malnutrition exposure. For the ‘*chronic mechanism*’, we use temporal variation in settlement density as a proxy for pathogen exposure. Both proxies are constructed using an extensive database comprising >110,000 ¹⁴C dates from >27,000 sites across the European and Mediterranean area. Model likelihoods (i.e. the probabilities of the allele frequency data; Figure ED2) indicate that settlement density and population fluctuations both provide significantly (accounting for multiple testing via Benjamini-Hochberg, see Table ED1) better explanations of LP allele frequency trajectories in prehistoric western Eurasia than spatiotemporally uniform selection (Figure ED3B-C), or milk use, providing support for both the ‘*crisis*’ and ‘*chronic*’ mechanisms (i.e. the LP allele data are 284 times or 689 times more probable under models of settlement density or population fluctuations, respectively, driving selection, than a model of constant selection).

We also considered the proportion of domestic and wild animals in faunal assemblages – constructed using >1,000,000 NISP (number of identified specimens) of 17 main meat-bearing taxa from 1,093 phases from 825 sites^{50,72} – as explanatory variables for LP allele frequency trajectories. However, it is not clear if exploiting more domestic animals would increase pathogen exposure, as domesticates tend to live in closer proximity to humans than wild animals⁷³, or if exploiting more wild animals would increase pathogen exposure, as greater pathogen diversity is expected for wild animals^{74,75}. Furthermore, a shift from domestic to wild animal exploitation might result from the economic instabilities associated with the ‘*crisis mechanism*’^{51,76}. Interestingly, the proportion of wild rather than domestic animals in archaeological assemblages provided higher model likelihoods (i.e. the LP allele data are 34 times more probable under a model of wild animal consumption driving selection, than a model of constant selection; Figure ED3D). This could be interpreted as support for either the ‘*crisis*’ or ‘*chronic*’ mechanisms, or be argued to counter the ‘*chronic*’ mechanism if prehistoric pathogen exposure was mainly from domesticates.

The prevailing narrative for the coevolution of dairying and LP has been a virtuous circle mechanism where LP frequency increased through the nutritional benefits and avoidance of negative health costs of milk consumption, facilitating an increasing reliance on milk that further drove LP selection. Our findings suggest a different picture. Milk consumption did not gradually grow throughout the European Neolithic from initially low levels, but rather was widespread at the outset in an almost entirely LNP population. We show that the scale of prehistoric milk use does not help to explain European LP allele frequency trajectories, and so selection intensities. Furthermore, we show that LP status has little impact on modern milk consumption, mortality or fecundity, and milk consumption has little or no detrimental health impact on contemporary healthy LNP individuals.

Instead, we find support for two related hypotheses: that LP selection was driven episodically and acutely by famine, and/or on a more continuous basis by synergies between pathogen exposure and the otherwise benign consequences of milk consumption in LNP individuals³⁸. We propose that these mechanisms would have applied in the disease and malnutrition-prone environment existing during the period of rapid increase in LP frequency but would not be expected to apply outside of these circumstances. This historical contingency is supported by the substantial increase in consumption of milk in contemporary China, where the vast majority of the population are LNP^{77,78}. In contemporary populations LP genotype associates with aspects of the gut microbiome⁷⁹, and we postulate that post-weaning childhood diarrhoeal disease mortality could have been increased in LNP individuals drinking milk. Over the period in which LP prevalence increased, the ratio of late childhood (5-18 years) to early childhood (2-5 years) mortality increased⁸⁰. The “*crisis*” and “*chronic*” mechanisms are, of course, not mutually exclusive, nor do they exclude other LP selection mechanisms, especially outside western Eurasia. We also test modern midday solar insolation incident on a horizontal surface⁸¹, and our maximum likelihood approach does indeed provide support for the *calcium assimilation hypothesis*³³, although it should be noted that solar insolation is strongly correlated with latitude, and may therefore be confounded by factors influencing the spatial spread of the LP allele, such as its origin location, ‘allele surfing’^{30,35}, or large-scale population movements²⁷. Other plausible hypotheses for selection favouring LP in Europe, such as milk as a relatively pathogen-free fluid³⁷, milk allowing earlier weaning and thus increased fertility⁸², milk galacto-oligosaccharide benefits for the colonic microbiome^{39,40}, or higher efficiencies of calorie production from dairy farming⁸³ are more difficult to assess. However, we note that the best proxy for all of these processes is milk consumption level, which itself provides no better explanation for LP allele frequency trajectories than constant selection through time. Therefore, the spatiotemporal patterns of LP selection in ancient Europeans do not reflect variation in their milk consumption. Instead, they map latitude, population volatility and settlement density; proxies for environmental conditions, subsistence economics and pathogen exposure, respectively. We note that – albeit in different configurations – these factors remain key drivers of human morbidity and mortality today.

Methods

Lipid residue analyses

Data, lipid extraction and analysis—Our lipid residue analysis draws on our SQL database of 13,181 archaeological potsherds from 554 sites, of which 6,899 sherds have yielded animal fat residues from georeferenced sites and dated phases (826 phases from 554 sites). This analysis represents c.30% new data, and c.70% collated from previously published studies^{1–87}.

Lipid residue analyses and interpretations were based on established protocols^{88,89}. Lipids were extracted from 1-3 g of cleaned potsherd and analysed using GC and GC-MS to determine their molecular composition. Compound-specific $\delta^{13}\text{C}$ values of fatty acids were determined using Agilent Industries 7890A gas chromatograph coupled to an Isoprime 100

isotope ratio mass spectrometer (GC-C-IRMS) for extracts identified as animal fats. Samples were introduced via a split/splitless injector in splitless mode onto a 50 m x 0.32 mm fused silica capillary column coated with a HP-1 stationary phase (100% dimethylpolysiloxane, Agilent, 0.17 μm). The GC oven temperature programme was set to hold at 40 $^{\circ}\text{C}$ for 2 min, followed by a gradient increase to 300 $^{\circ}\text{C}$ at 10 $^{\circ}\text{C min}^{-1}$, the oven was then run isothermally for 10 min. Helium was used as a carrier gas and maintained at a constant flow of 2 mL min^{-1} . The combustion reactor consisted of a quartz tube filled with copper oxide pellets which was maintained at a temperature of 850 $^{\circ}\text{C}$. Each sample was run at least in duplicate. Instrument stability was monitored by running a fatty acid methyl ester standard mixture every 2 or 4 runs. The $\delta^{13}\text{C}$ values are the ratios $^{13}\text{C}/^{12}\text{C}$ and expressed relative to the Vienna Pee Dee Belemnite, calibrated against a CO_2 reference gas injected directly in the ion source as two pulses at the beginning of each run. Instrumental precision was 0.3 ‰. Data processing was carried out using Ion Vantage software (version 1.5.6.0, IsoPrime).

^{13}C proxy for milk exploitation—The $\delta^{13}\text{C}$ values of the $\text{C}_{16:0}$ and $\text{C}_{18:0}$ fatty acids from more than 170 modern ruminant adipose and dairy fats taken from animals raised in Europe, Eurasia and Africa, reveal a consistent difference in the $\delta^{13}\text{C}$ values of the $\text{C}_{18:0}$ fatty acid, which relate to the different biosynthetic origins of this fatty in the two fat types^{6,90}. The result is that $\delta^{13}\text{C}$ values of the $\text{C}_{18:0}$ fatty acid in milk is always depleted compared to the $\text{C}_{18:0}$ fatty acid in ruminant adipose fats by on average 2.3‰⁶. This difference allows archaeological ruminant fats extracted from pottery to be assigned as either milk or adipose fats.

Initial reference fats were taken from animals grazing in a pure C_3 plant dominated pasture in the UK and archaeological investigations of dairying in historically pure C_3 regions can be achieved by comparisons with the raw $\delta^{13}\text{C}$ values, e.g. refs^{6,90}. However, in regions where C_4 plants are present and other environmental factors, e.g. high aridity, affect the raw $\delta^{13}\text{C}$ values, the ^{13}C values (i.e. $^{13}\text{C} = \delta^{13}\text{C}_{18:0} - \delta^{13}\text{C}_{16:0}$) are used to remove the environmental effects, e.g. refs^{91,92}. For modern reference fats, ruminant milk fats are distinguished from ruminant adipose fats in displaying ^{13}C values $< -3.1\text{‰}$, ruminant adipose fats plot between -3.1 and -0.3‰ , with non-ruminant fats plotting at $> -0.3\text{‰}$. Individual archaeological pottery lipid extracts are assigned to fat type based on their ^{13}C values using the ranges defined by the reference fats.

Animal fats extracted from potsherds are categorised as containing milk lipids if their ^{13}C ($= \delta^{13}\text{C}_{18:0} - \delta^{13}\text{C}_{16:0}$) values are below the threshold -3.1‰ , or non-milk otherwise⁹². Although this threshold choice influences the absolute proportion estimates, it has almost no influence when evaluating the fluctuations in milk use through time since the relative proportions will be largely unaffected (see Methods Fig 1 below). Indeed, even if the exact number of sherds containing dairy fat residues were known, this could not be used as a proxy for milk proportion in overall diets due to biases in pottery use. Similarly, our conclusion that milk exploitation was widespread throughout the Neolithic is also based on the observation that the proportion of sherds with dairy fat residues were similar to the Bronze Age.

Chronology—Archaeological sherds are associated in the MySQL database with specific site phases. Each phase is assigned a uniform date range using published start and end dates from archaeological site reports. If unavailable, we used calibrated⁹³ radiocarbon dates to construct phase models in OxCal⁹⁴, and used the mode of each boundary posterior distribution as start and end dates. In cases where neither of these sources were available (10% of phases), phases ‘borrow’ their chronology from the geographically closest site-phase that has the same associated culture. Date ranges of site-phases are reasonably constrained (75% less than 580 years).

UK Biobank analysis

Data—UK Biobank^{95,96} is a large prospective cohort study of approximately 500,000 UK participants aged 37-73 years at recruitment (2006-2010). The study collected a wide-range of measures including demographics, health status, lifestyle, cognitive function, mental and physical health and molecular data such as genetic and biomarkers. UK Biobank received ethical approval from the Research Ethics Committee (REC reference for UK Biobank is 11/NW/0382). All analyses were performed under application 16729.

Dairy consumption—Multiple measures of milk consumption were evaluated through this study.

Milk servings: Participants were asked: how many glasses/carton/ 250ml of milk (excluding milkshakes) did you consume yesterday? (field 100520) and how many glasses/carton/ 250ml of yogurt drinks, flavoured milk or milkshakes did you consume yesterday? (field 100530). These measures were only asked if participants drank some milk the previous day and therefore there was no zero servings value. To reduce missingness, mean servings were calculated from five repeated measures taken in 2009-12.

Dairy milk preference: Participants were asked at baseline: What type of milk do you mainly use? (field 1418). From this variable binary non-dairy vs dairy consumption was derived: soya and never/rarely have milk vs full cream, semi-skimmed and skimmed.

Lactose-free diet: Participants were asked: Do you routinely follow a special diet? Respondents answering —Yes” to diet for lactose intolerance on any of the five repeated measures undertaken 2009-12 were compared against participants answering —No” to all non-missing responses.

Genetic data: We focused on the major European lactase persistence variant located upstream of the coding gene promotor (rs4988235, LCT -13910*T)⁹⁷. The lactase genotype showed strong departure from Hardy-Weinberg equilibrium (HWE) in UK Biobank white British participants (Table ED2; $\chi^2=77.31$; $P=1.46 \times 10^{-18}$) using the HardyWeinberg R-package (1.6.3) (ref. ⁹⁸). This finding could arise from non-random mating, clinical ascertainment bias, genotyping error, or population stratification/admixture⁹⁹. The latter was mitigated as far as reasonably possible using a homogenous population which was clearly effective when considering the more extreme HWE violation in “any other white background’ group (Table ED2; $\chi^2=422.52$; $P=6.9 \times 10^{-94}$). HWE violation was also

observed in gnomAD¹⁰⁰ which contains genotype frequencies on 32,263 non-Finnish Europeans using exome/whole genome sequencing (Table ED2; $\chi^2=235.75$; $P=3.32 \times 10^{-53}$). Sequencing and array technologies have distinct error profiles and therefore technical artefact is an unlikely explanation.

Lactase gene variant crude association with dairy consumption—Unadjusted genotype frequencies stratified by dairy consumption were calculated from an unrelated white British subsample of UK Biobank prepared according to Mitchell et al.¹⁰¹.

Lactase gene variant association with health outcomes—Variant association with health outcomes was performed using an unrelated white British subset of UK Biobank for the main analysis and within-family estimates for sensitivity analyses. Time-to-death was estimated using a Cox proportional hazards model. All-cause mortality was derived from field age-at-death (40007). The following fields within the UK Biobank were used: Body Mass Index (21001); Father's age at death (1807); Heel bone mineral density (78); IGF-1 (30770); Mother's age at death (3526); Number of children fathered (2405); Number of live births (2734); Standing height (50); Vitamin D (30890). All models assumed additive inheritance and were adjusted for age, sex and top 40 genetic principal components. Within-family estimates were produced using panel regression as previously described¹⁰². All outcomes were collected at baseline.

Estimate of assortative mating on dairy consumption—To determine if milk consumption influences mate choice and therefore invalidates HWE assumptions⁹⁹, we estimated the spousal LP genetic correlation (Table ED3) adjusted for age, the first ten genetic principal components, partner age, and partner first ten genetic principal components. Under an additive linear model there was very weak evidence in support of assortative mating on lactase persistence (0.004 mean increase in partner LP genotype per increase in individual LP genotype [95% CI -0.002, 0.011]). However, a single allelic copy of LP is sufficient to produce the observable phenotype (milk intake; Table 1 main text) and therefore we considered a dominant inheritance model (imputed variant dosage capped at one; rs4988235 GG vs GA & AA). Using logistic regression, we found milk consumers were at 10% increased odds of selecting a milk drinking partner (mean increase of 1.10 OR [95% CI 1.00, 1.22] partner having one or more copies of LP among LP individuals). The effect was consistent under sensitivity conditions additionally adjusting for top 40 genetic principal components (mean increase of 1.11 OR [95% CI 1.00, 1.22] partner having one or more copies of LP among LP individuals) reducing the possibility partner selection was driven entirely by population stratification.

We also found a weak effect of the variant on the number of children fathered (0.01 SD [95% CI 0.00, 0.01]; Figure 4, main text) consistent with the variant improving overall fitness which could in-part explain the positive selective pressure on the locus and observed violation of HWE.

Spouse-pairs were derived and validated in a European subsample of UK Biobank ($n = 47,459$) supplied by Dr Laurence Howe, MRC IEU¹⁰³. Analyses were restricted to spousal-pairs with complete data ($n = 46,560$).

All regression models were implemented in R (v3.6.1).

Ancient DNA Analyses

Data—We collated published BAM files from 2,999 ancient Eurasian individuals^{104–154}, out of which 1,786 had the European LP single nucleotide polymorphism (SNP) covered at least once (read depth: span 1 to 128-fold, average 7-fold). All genomes came aligned to the GRCh37/hg19 human reference assembly, but for the Tyrolean Iceman (hg18). Relevant geographic and temporal annotation was extracted from David Reich’s aDNA compendium v44.3 (ref. ¹⁵⁵), see Figure 3 for a representation of the full dataset. For the joint analyses of genetic and ecological data, we restricted this dataset to those individuals spatiotemporally overlapping the ecological data (four geographic regions: ‘British Isles’, ‘Rhine-Danube axis’, ‘Mediterranean Europe’, and the ‘Baltic region’; 8000-2500 BP), leaving 2,162, out of which 1,293 had the lactase locus covered at least once (read depth: span 1 to 128-fold, average 7-fold).

We extracted the pileup at the position of the European LP SNP (rs4988235; in hg19: chromosome 2, position 136608646; hg18: chromosome 2, position 136325116) with default quality cutoffs using Samtools¹⁵⁶. For sites with read depth at least two, we called the diploid genotype with the highest likelihood, for sites covered only once, only a single allele was called. Exceptions are individuals PEN001_real2 (ref. ¹⁴⁴) and Klei10 (ref. ¹²²), which each have one out of four reads with the derived allele. However, as discussed in the respective publications, the ages of the samples suggest the derived alleles are rather the consequence of post-mortem damage, and we therefore consider both of them as homozygous ancestral.

Likelihood of an ecological proxy variable driving LP fitness advantage—Many phenomena have the potential to influence LP allele frequency trajectories in each of our geographic regions, including selection, migration, genetic drift and population structure. We explore just one of these factors in isolation – selection – in order to test if the observed archaeological allele frequencies are best explained purely under a null model of constant selection, or might be partly explained by a model whereby the intensity of selection varies through time in accordance with a hypothesised ecological driver. While selection strength cannot be observed directly, population genetic models describe its effect on expected allele frequencies. Given the set of ecological proxy variables that we hypothesise may act as selective agents we can ask if fluctuating selection models based on these variables fit the genetic data better than a null model of constant selection strength. If a fluctuating model fits best, we may infer that the ecological proxy is linked to the true selective agent.

We obtain a likelihood equation in the following way. Say $m(t)$ is a time series over time t , with $m(t) \in [0,1]$. We parameterise its effect on selection strength s as $s(t) = b \cdot m(t)^{\frac{1}{a} - 1}$, where $b \in [0, 1]$ is the maximal selection coefficient modulated by a factor that depends on the time series and an exponent $a \in [0, 1]$. Note that with $a = 1$ the model simplifies to one of constant selection strength.

As selection on lactase is strong, we assume a deterministic allele frequency trajectory, ignoring random drift. We assume a generation time of 28 years. In case of an additive model for selection—corresponding to relative fitnesses $1 + 2s$, $1 + s$, and 1 for homozygous derived, heterozygous, and homozygous ancestral genotypes respectively—we approximate the expected allele frequency after t generations (divide by generation time to scale to years) by $\frac{y_0}{y_0 + (1 - y_0)e^{-st}}$ with an additional model parameter y_0 for the initial allele frequency at time point \square_0 (here set at 8000 BP). This avoids the challenges of estimating the date of the LP mutation by assuming it was present in the population at \square_0 at some unknown frequency, y_0 . Moreover, this avoids modeling the lowest frequency part of the allele trajectory where drift is strongest.

In most cases, $m(t)$ will be piecewise constant over time windows in the order of a hundred years, meaning that $s(t)$ is piecewise constant as well, and allele frequencies can be computed in between these boundaries with the equation above setting the initial frequency of later time intervals to the last one of the preceding time interval.

The dominant model—corresponding to relative fitnesses $1 + s$, $1 + s$, and 1 for homozygous derived, heterozygous, and homozygous ancestral genotypes respectively—is considered here as well – as the lactase persistence phenotype has been shown to be dominant. It requires numerical optimisation of an approximation as no exact expression for $y(t)$ as a function of y_0 , s and t exists. $y(t)$ can be obtained by keeping y_0 , s and t constant and adjusting $y(t)$ until equation $t = \frac{1}{s} \left[-\frac{1}{1 - y_0} + \ln\left(\frac{1 - y_0}{y_0}\right) + \frac{1}{1 - y_t} - \ln\left(\frac{1 - y_t}{y_t}\right) - s \cdot \ln\left(\frac{y_0}{y_t}\right) \right]$ is satisfied¹⁵⁷. As above, this allows us to compute expected deterministic allele frequency trajectories for piecewise constant selection strengths. Note that due to the parametrisation of fitness, the dominant selection coefficient has to be multiplied by a factor 2 to be comparable to the additive model.

For an expected allele frequency trajectory over the entire time range under one of the above inheritance models, the log likelihood given k observed ancestral alleles at time points t_i and n derived alleles observed at time points t_j is computed as $\sum_{i=1}^k \ln(1 - y(t_i)) + \sum_{j=1}^n \ln y(t_j)$. We were able to construct ecological proxy variables for four distinct regions, with different time series $m(t)$ and therefore different expected allele frequency trajectories. In order to analyse these regions jointly, log-likelihoods were summed over all four regions, to result in a single optimal parameter combination across all regions.

For a given time series $m(t)$ we optimised the model parameters y_0 (initial allele frequency at time point 0), a and a (with $a = 1$ fixed for the constant selection strength model) using the ‘JDEoptim’ function from the ‘DEoptimR’ library¹⁵⁸ in R¹⁵⁹. We chose the best parameter combination from six independent runs, three with and three without initialising JDEoptim with the parameters found for the constant selection model.

Finally, statistical model comparison was performed by computing \square -values obtained from a likelihood ratio test accounting for the different number of parameters between constant and fluctuating models (two and three respectively). We controlled the false discovery rate in the multiple testing of different models with the Benjamini-Hochberg procedure, i.e. ordering

the α -values, $\alpha_1, \alpha_2, \dots, \alpha_n$ and declare a test of rank α non-significant at level δ if $\alpha_n > \alpha \frac{\alpha}{\alpha} \dots$

Power analysis—We analysed the power of our approach to estimate parameters and detect ecological proxies linked to selection strength via simulations. We chose to focus on milk exploitation, in particular to assess the robustness of our finding that milk is unlikely to drive selection on the LP allele.

First, we simulated genotypes under nine different model parameter combinations, with three replicates per combination, sampling a matching number of alleles (one or two) at the corresponding time points in the real data. Figure ED4 shows the results for all combinations of $\alpha \in \{0.02, 0.035, 0.05\}$ and $\beta \in \{0.2, 0.6, 0.8\}$, with an initial frequency y_0 fixed at 0.005. We observe that both parameters can be estimated accurately when $\alpha > 0.02$ or $\beta > 0.25$. Models with small values for α or β are most challenging as both lead to small selection coefficients on average (small values α for lead to very few bursts of high selection over a background of otherwise weak selection, see for example Figure ED3B) and therefore a generally low number of sampled derived alleles. Figure ED5 illustrates this phenomenon, where absolute errors in the estimates of α and β for three replicate simulations per parameter combination above, repeated independently for three different initial frequencies $\alpha_0 \in \{0.0005, 0.005, 0.01\}$, are plotted against the number of simulated derived alleles. High estimation errors are exclusively found when few derived alleles are simulated, as the latter are responsible for important likelihood differences between models with appreciable LP allele frequencies. The number of derived alleles in our dataset seems to be high enough to estimate α with high and β at least with intermediate accuracy. Besides the estimation of actual model parameters, we quantified the power to select a model with milk as a driver over a constant selection model. For the same set of simulations underlying Figure ED5, we show the likelihood differences between a model of constant selection and one where milk exploitation drives selection strength on the derived LP allele in Figure ED6. With less than 30 derived alleles, which is the number we observe in the actual data, only 20% of the likelihood differences pass the significance threshold, compared to 81% for simulations with at least the same number of derived alleles (51% overall), where we restricted the set of simulations only to those with an estimated parameter α above 0.95 (values close to one effectively lead to constant selection models and therefore a likelihood difference close to zero). We are therefore confident that if milk acted as a driver of selection strength in our data we would at least find a meaningfully increased likelihood.

Second, we assessed the impact of noise in the ecological proxies, here exemplarily and most importantly in the context of this study on milk exploitation. To simulate inaccuracies, we multiplied each constant piece of the milk exploitation proxy by a random number uniformly drawn from the interval $[0.5, 1.5]$, leading to a ‘noisy’ version which differs from the original values on average by 0.091 (corresponding to ~11% of the milk variable’s full range from 0 to ~0.8; maximum deviation 0.32). Figure ED7 compares parameter estimates and likelihoods with the values found in the corresponding simulation shown in Figure ED4. While there are outliers with noticeable deviation when $\alpha = 0.25$ (most challenging to distinguish from a constant selection model as discussed above), the remaining parameter

estimates are barely affected, and none of the likelihoods change across the significance threshold. Therefore, we consider our approach robust against moderate levels of noise in the milk exploitation proxy, and more generally in other time series.

Lastly, we sought to quantify the effect that drift—which we are not explicitly modelling—may have on our inferences. We repeated the experiments shown in Figures ED4-ED6, however, simulating allele frequency trajectories with fluctuating selection and drift as the basis from which alleles are drawn with the sampling strategy described above that emulates our real aDNA data (drift simulations only with initial frequency $\Delta_0 = 0.005$). We used the ‘learnPopGen’ R library¹⁶⁰, and simulated two levels of drift by setting the effective population size to $N_e \in \{1,000, 10,000\}$ (generation time implemented by extending allele frequencies per generation to piecewise constant frequencies lasting 28 years). We observe that the ability to accurately infer N_e is only mildly affected, whereas the effect on s is stronger (Figure ED8). This is in line for example with Jewett et al.¹⁶¹, where the authors find limited benefit to explicitly model drift for the inference of selection coefficients. Plotting the same data differently shows that the relationship with the number of simulated derived alleles continues to hold, although the accuracy of estimates drop with stronger drift even at high numbers of simulated derived alleles (Figure ED9). Importantly, the ability to detect significant likelihood differences in the presence of drift is not affected (Figure ED10), as detailed in Table ED4. Hence, we consider our modelling robust against mild levels of drift and a deterministic model appropriate, especially as selection coefficients are known to have been high on the derived LP allele and as our geographic regions are large enough to warrant high effective population sizes.

In conclusion, our approach performs well at estimating parameters, especially when the number of derived alleles is at least that in the real aDNA data we curated for this paper, and most importantly has the power to select a fluctuating over a constant selection model, even in the presence of moderate drift and noise in ecological driver variables.

Ecological Proxy Variables: hypothesised drivers of LP selection—We generate five ecological variables as proxies for hypothesised drivers of LP selection. Each variable is generated for four geographic polygons which overlap spatially and temporally with our ancient genetic data (‘British Isles’, ‘Baltic region’, ‘Rhine-Danube axis’ and ‘Mediterranean Europe’). We make no assumption about the direction of the possible relationship between each variable (V) and the selection coefficient - i.e. if they are positively or negatively correlated. Therefore, we also generate a set of inverse variables, which can be notionally considered as a reflection, for example a variable that ranges between 0 and 1 will have an inverse variable between 1 and 0.

Radiocarbon dates—Two of the five ecological variables (Residential density, and fluctuations in population levels) were constructed directly by utilising an extensive database comprising >110,000 ¹⁴C dates which we compiled from over 1,000 published sources including CalPal¹⁶², BANADORA¹⁶³, RADON¹⁶⁴, EUROEVOL¹⁶⁵, Wales and Borders radiocarbon database¹⁶⁶, Scottish Radiocarbon Database¹⁶⁷, Balsera et al.¹⁶⁸ and the Palaeolithic Europe Database¹⁶⁹, which provided the majority of radiocarbon dates. A summary of the radiocarbon dates used within our four polygons can be found at

<https://github.com/AdrianTimpson/2020-03-03523A> and a full list of sources is available on request.

Residential density (clustering)—Under the assumption that dwelling proximity increases the potential for the spread of disease in a population, our ‘chronic’ mechanism hypothesises that periods and regions of greater residential density would tend to suffer more from diseases, providing greater selection on LP. We construct a residential density statistic (RDS) from the site locations of our radiocarbon database. The RDS is influenced neither by the number of archaeological sites (which is heavily biased by differential sampling, and a general increase through the Neolithic from population growth), nor by geographic structure in the site locations (caused by features such as islands and mountains). Instead, our RDS uses the distribution of pairwise distances between all sites in a region as a null expectation, and then calculates how the distribution of pairwise distances in each time slice deviates from this expected distribution. We achieve this by first generating the Empirical Cumulative Distribution Function (ECDF) of pairwise distances of all sites ($ECDF_{all}$), then for a single time slice we generate the ECDF of pairwise distances of sites that fall within that time slice ($ECDF_t$). We then calculate the RDS in that slice as $sum(ECDF_t - ECDF_{all})$. This is repeated for each time slice, giving a vector of RDS values. Given there is substantial chronological uncertainty for each site, we also use associated radiocarbon dates to generate a Summed Probability Distribution (SPD) after calibrating through IntCal13 (ref. ⁹³). We use the 99% quantiles of this SPD as a conservatively wide date range for the site. We then uniformly sample a date from this range, in order to assign each site to just one time slice. The entire process is repeated 500 times to generate 500 RDS vectors. This allows CIs to be generated that incorporate the chronological uncertainty in the dataset, and we use the mean of these 500 replicates as the final time series in the LP model.

Animal exploitation (proportion of wild or domestic)—Fluctuations between domestic and wild animal exploitation for meat have the potential to inform on various economic, social and food production changes. For example, we might expect an increase in the proportion of domesticates to be associated with greater animal husbandry, and increased contact with animals could lead to a greater probability of zoonotic diseases, and therefore greater selection. Conversely, we might expect periods of famine from failure of agriculture to result in a return to exploiting wild resources, thus a decrease in domestic animals might correlate with periods (and regions) with greater selection. We extract NISP counts of the main meat bearing taxa for domestic (*Bos taurus*, *Sus scrofa domestica*, *Ovis aries*, *Capra hircus*, *Ovis aries / Capra hircus*, *Equus caballus*) and wild (*Bos primigenius*, *Sus scrofa scrofa*, *Cervus elaphus*, *Alces alces*, *Rupicapra rupicapra*, Cervidae, *Oryctolagus cuniculus*, *Lepus europaeus*, Lagomorpha, *Equus ferus*) from the EUROEVOL¹⁷⁰ and OSSK¹⁷¹ databases. Therefore, for a given time slice the ‘domesticates’ and ‘wild’ NISP counts are used to calculate a proportion of domesticates.

Fluctuations in population levels—We utilise our radiocarbon database and the R package ADMUR directly model the underlying broadscale population dynamics as the combination of exponential population growth with power law taphonomic loss. A Summed Probability Distribution (SPD) was also generated, and the residual difference between the

short term fluctuations of the SPD and the long term trend of the model was used as the detrended proxy for short term fluctuations in human presence through time. This was achieved independently for each of the four geographic polygons, after all radiocarbon dates were calibrated through the *intcal20* curve⁹³ Finally, we normalise these residuals to a range between 0 and 1 globally, by scaling each variable by the smallest and largest values found across all polygons. In all cases to adjust for ascertainment bias, radiocarbon dates in a site-phase were first aggregated and normalised, so that the total probability mass for each site-phase was 1, no matter how many radiocarbon dates at a site-phase.

Solar insolation—We calculate mean annual solar insolation at 0.5 by 0.5 degree resolution using modern data (1983 to 2013) from NASA’s midday insolation incident on a horizontal surface¹⁷² (W/m^2). Values at each grid point are then used to calculate a single mean value for each of the four geographic polygons. Therefore unlike the previous ecological variables that each comprise three time-series, solar insolation (and its inverse) are not time variable. No doubt insolation would have fluctuated over the study period, but the magnitude of this variation is trivial compared to the variation between polygons. These values are then normalised to a range between 0 and 1 by dividing by the Earth’s single greatest mean annual solar insolation value of $867.90 \text{ W}/\text{m}^2$.

Time-series plots and interpolation maps—We account for three sources of uncertainty when estimating frequencies from count data (LP and LNP alleles, potsherds with and without dairy fat residues, domestic and wild species NISP). Within any time-slice we have multiple site-phases, each of which has integer counts of presence and absence. Sample sizes vary hugely between sites (potsherds between 1 and 121, NISP between 1 and 61,497), and our objective is to fairly estimate the ‘underlying’ frequencies of these count data across all these site-phases. We ensure each site contributes fairly to this estimate, by weighting by the precision of each site’s frequency estimate (a function of sample size n , where the weight is defined by $1 - 1/\sqrt{(n + 1)}$).

In addition, to fairly incorporate in our estimate the uncertainty both from small sample size and chronology, we adopt a three-stage sampling process in our estimate, which is repeated 5,000 times in order to also find the Maximum a Posteriori (MAP) and Credible Intervals. The first stage randomly samples a single frequency from a Beta distribution, where the two shape parameters are the observed presence and absence counts in the site-phase. This includes an additional one count of each as a uniform prior. The second stage randomly samples a date from the site-phase’s date range. This then allows us to assign each phase to exactly one time-slice. The third stage then calculates the weighted average frequency of the site-phases (in each time-slice), weighted according to their sample size as explained above. Where a phase spans two (or more) time slices, its contribution to each slice is weighted accordingly.

Interpolated maps of the frequency of dairy fat residues (Fig 2) were achieved with a novel kernel density approach that generates both the interpolated frequencies using colour hue, and confidence in the interpolation using colour saturation. We constructed a 2D Gaussian kernel for each site-phase, the magnitude of which was weighted by the precision of the estimate, using $1 - 1/\sqrt{(n + 1)}$ where n is the number of sherds that have yielded animal

fats. The frequency of dairy residues at any geographic point was then calculated as the average of the proportion of sherds containing dairy fat residues over the total number of sherds yielding residues at a given site-phase, weighted by the probability density function (pdf) of each site-phase's kernel at that point. Therefore, the influence each site-phase has on any interpolated point on the map depends primarily on its geographic distance from that point, but is also influenced by the error on its frequency estimate. This second influence is small in comparison, since the most extreme difference in the relative contribution of sites is only threefold (0.909 where $n = 121$ compared to 0.293 where $n = 1$). The combined surface of 2D Gaussian kernels (for all site-phases) generated during the interpolation then determines the colour saturation, to illustrate geographic regions where there is an absence of data. Conceptually this approach describes the idealised process of shooting paintballs at a grey map. A paintball corresponds to the information content at a site-phase, such that its central position is determined by the site's latitude and longitude; hue is determined by the dairy fat frequency; and size of paintball is determined by the precision. Two further parameters are required. Firstly, the bandwidth of the kernel, which determines the spread of each paintball. Secondly, a saturation exponent which determines the hue of each paintball (the amount of information content). Both parameters were estimated using a cross-validation approach that partitioned the data into 80% training and 20% test, repeated 1,000 times. For each replicate, the training partition was used to generate interpolated maps (given a proposed bandwidth and saturation exponent), and a comparison was made at the locations of the test partition between the predicted values and the observed values. This comparison utilised a summary statistic that accounts for both the interpolated dairy residue frequencies, and the confidence (saturation). A good answer (predicted frequency close to the observed frequency) is better than an uncertain prediction (low saturation) which is better than a bad answer, therefore we seek to maximise saturation where predicted frequencies are accurate, and minimise saturation where predicted frequencies are poor. Therefore our summary statistic was the magnitude of the difference between saturation and prediction accuracy, which was minimised when bandwidth = 6.18 and the saturation exponent = 0.0538, see methods Fig. 2.

Extended Data

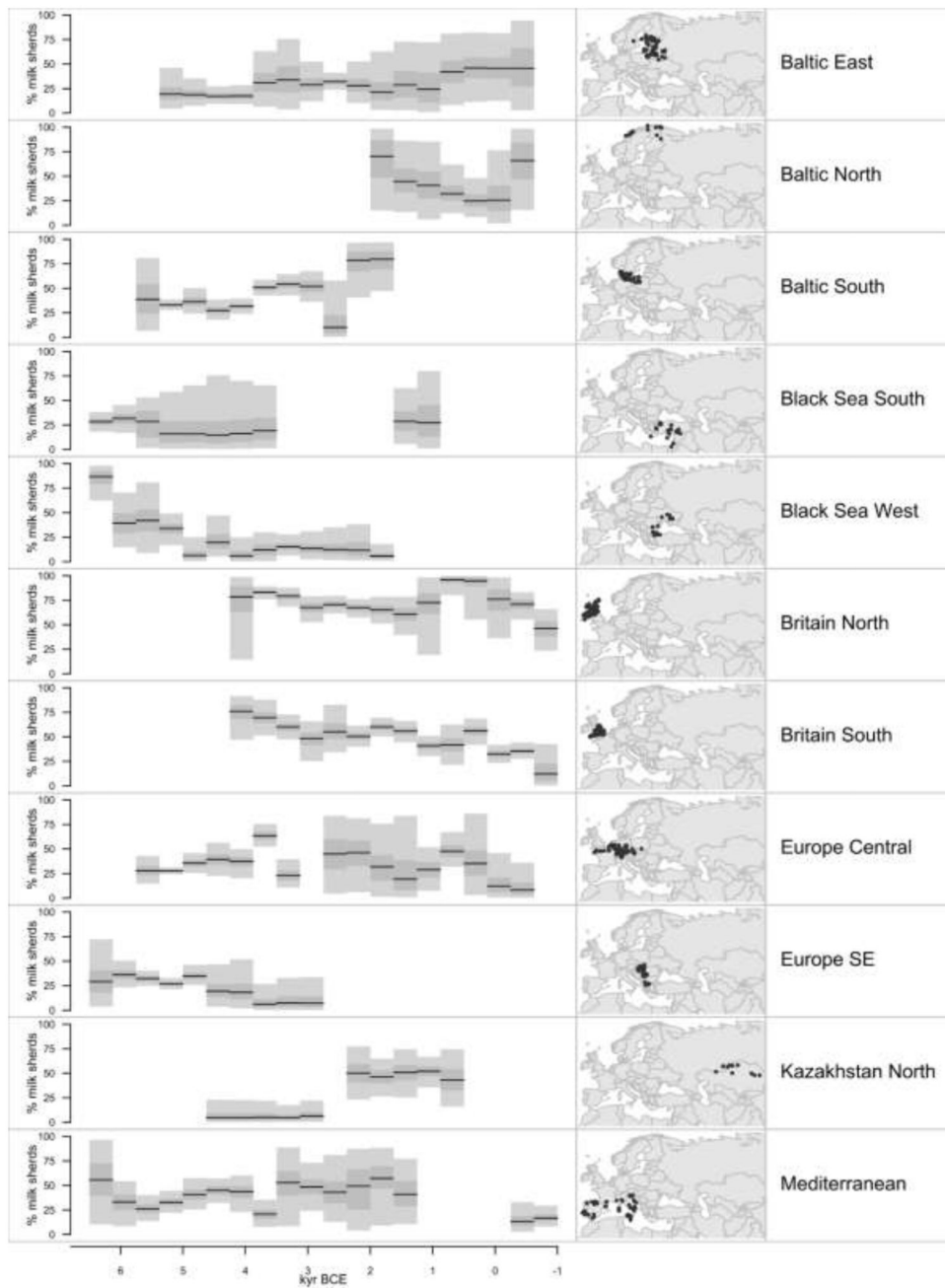


Figure ED1. Regional fluctuations in milk use throughout European prehistory
 Percentage of milk fats through time, calculated using all animal fat residues. Grey bars and black lines illustrate 95%, 50% CI and MAP in each time slice, using a uniform prior.

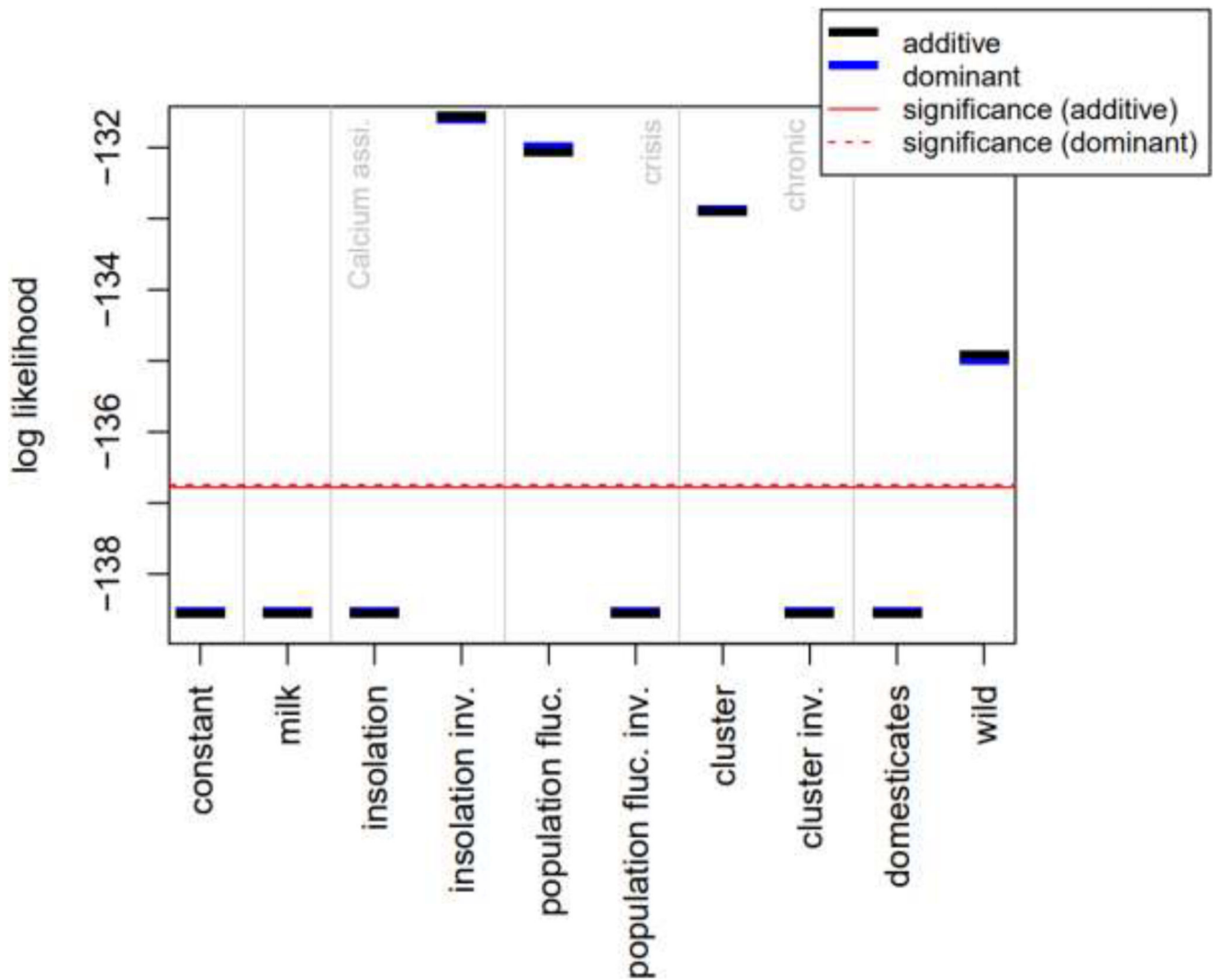
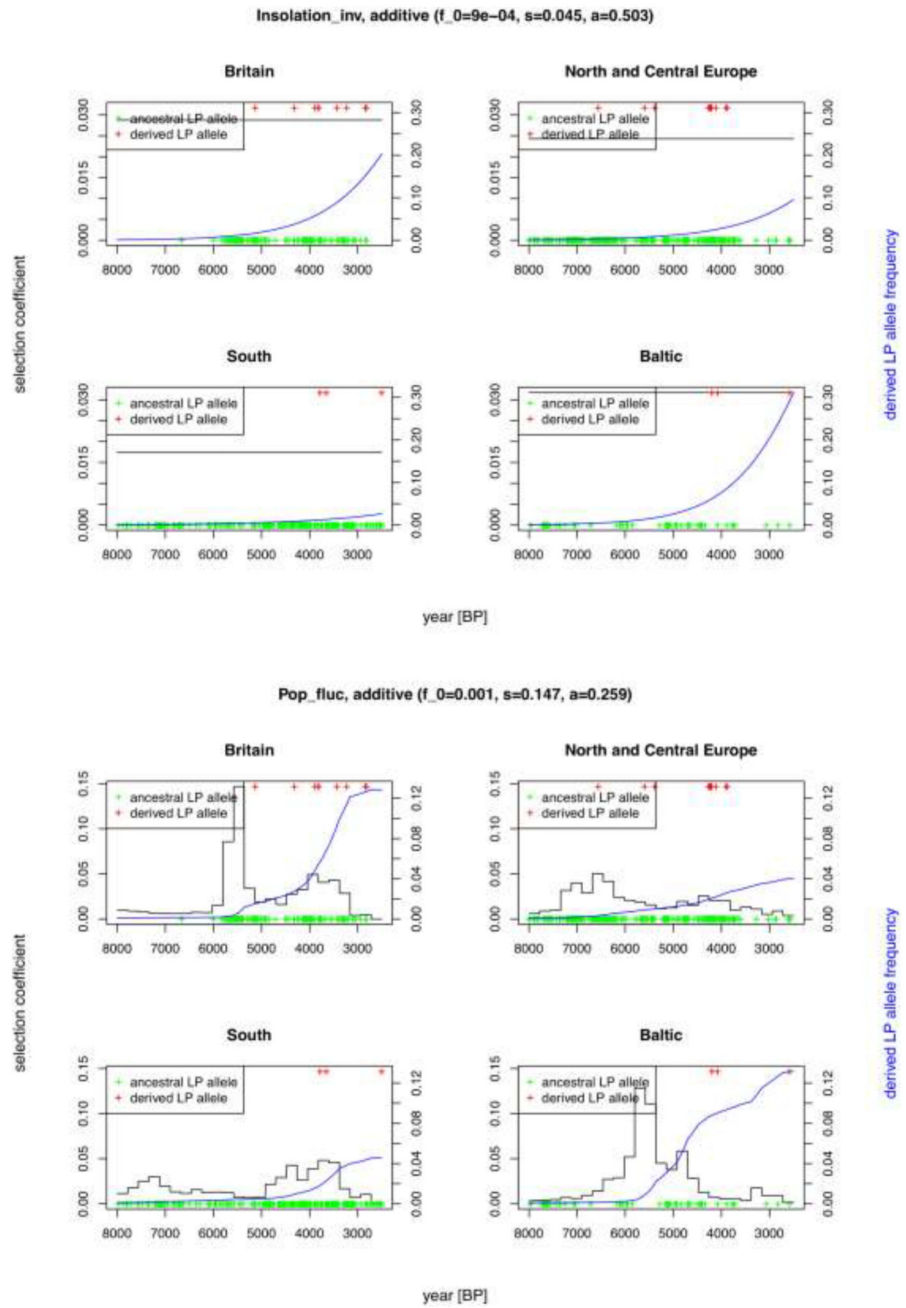


Figure ED2. Summary of model selection results for the tested ecological time series.

Inverse solar insolation, fluctuations in population level, and residential density yield models significantly better than a null model of constant selection. See Table ED1 for corresponding parameter estimates, and multiple testing correction (no change in the set of significant models). *Abbreviations:* assimilation (assi.), inverse (inv.), fluctuation (fluc.)



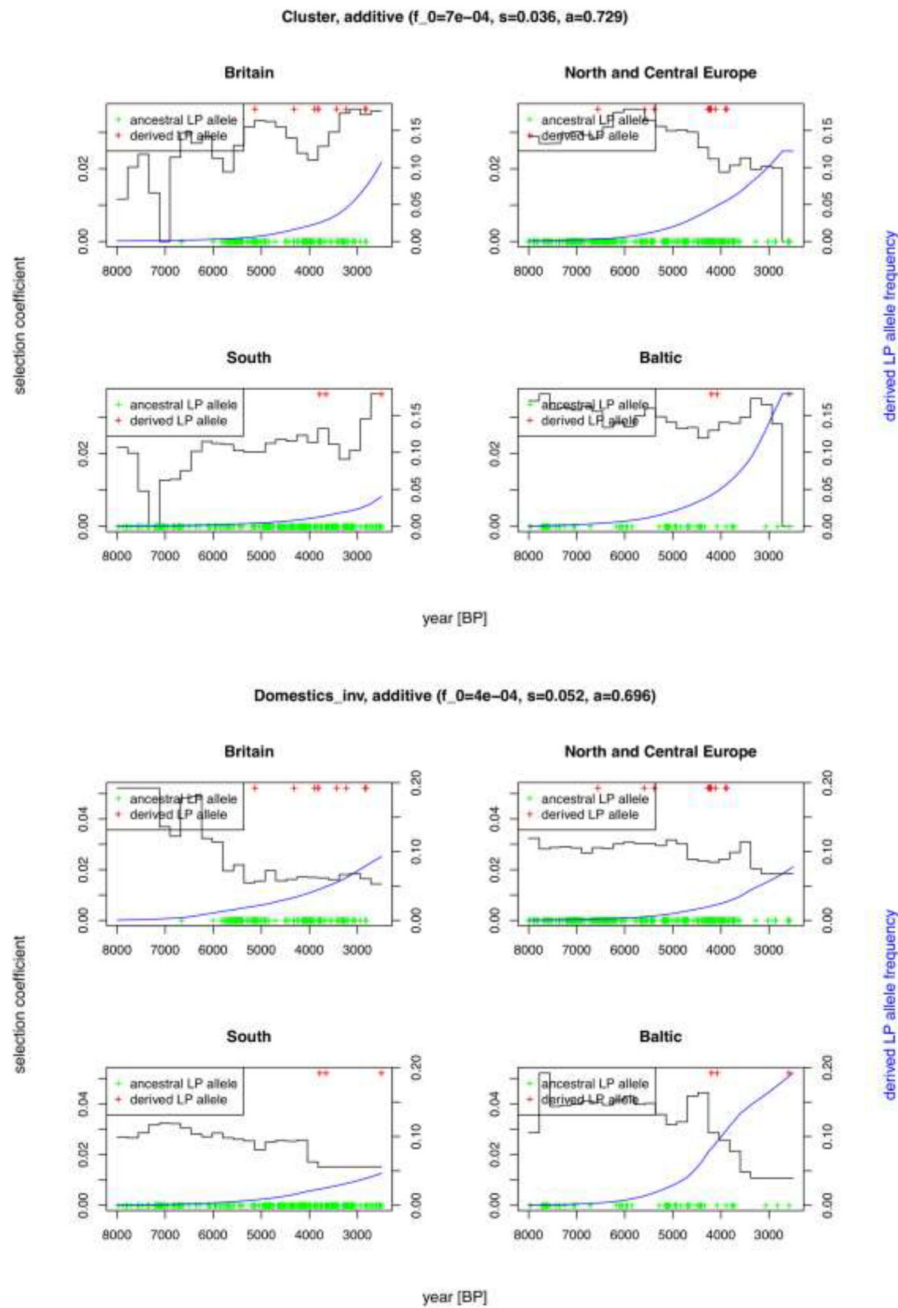


Figure ED3. A-D—Most likely models fitted to four ecological proxy variables yielding likelihoods significantly better than a constant selection model.

Although LP is generally thought of as a dominant trait, we only show the additive model results as the parameter estimates barely differ. *Abbreviations:* inverse (inv.), population (pop.), fluctuation (fluc.)

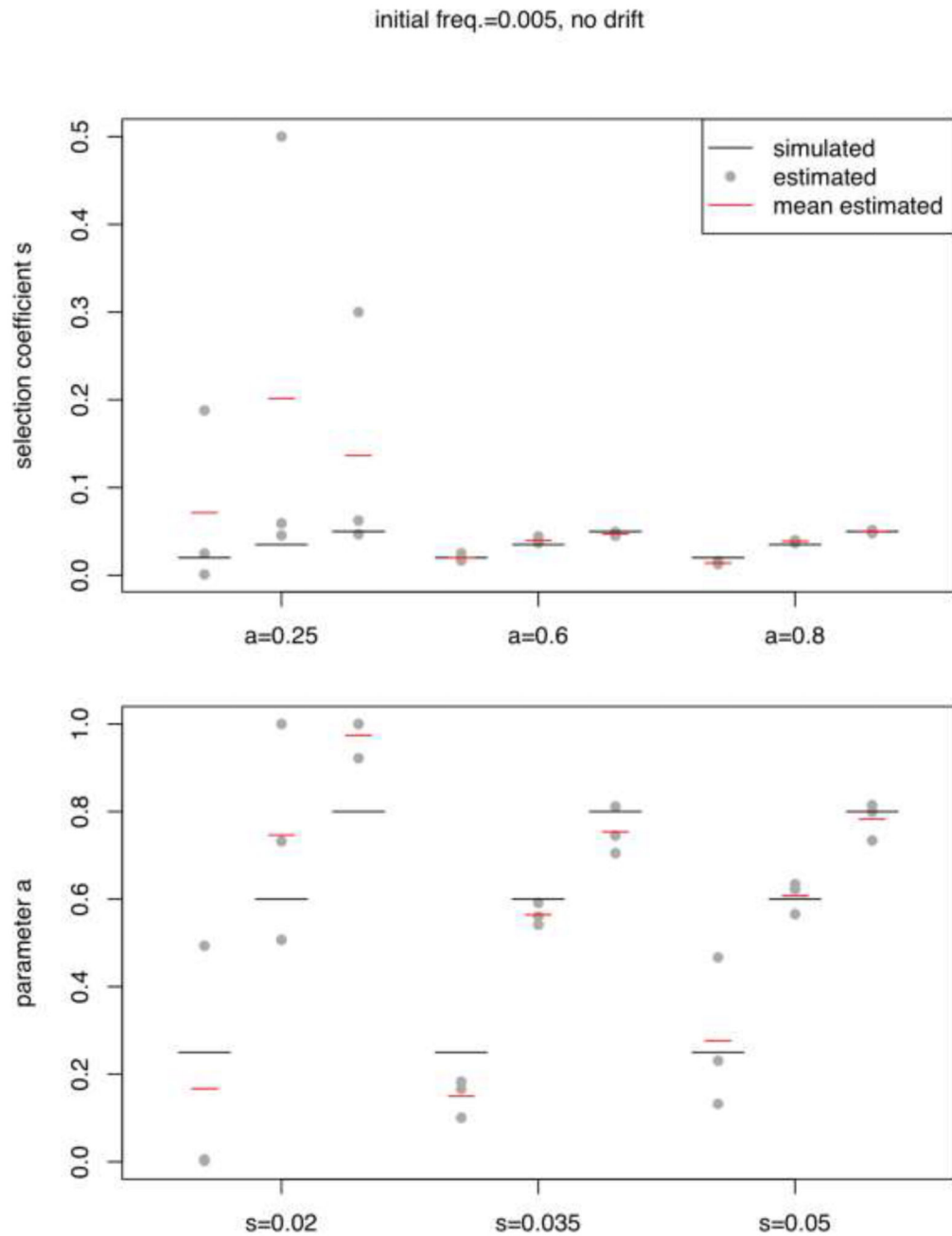


Figure ED4. Parameter estimation accuracy without drift.

True and inferred parameters \square and \square for three replicates of each of nine parameter combinations, simulated based on the milk exploitation ecological proxy and with initial allele frequency. $\square_0 = 0.005$. Abbreviations: frequency (freq.)

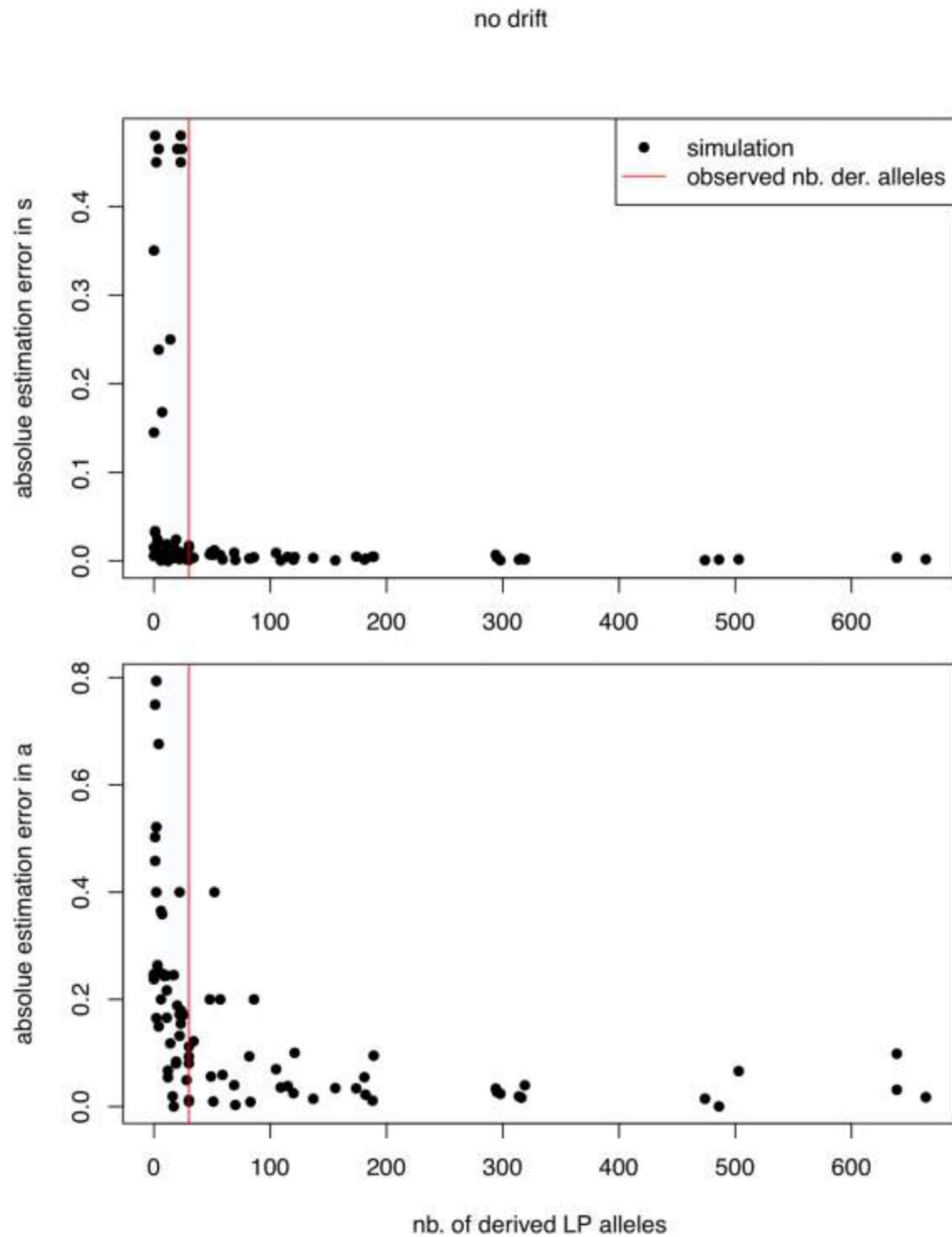


Figure ED5. Parameter estimation accuracy in relation to the number of derived alleles simulated without drift.

The simulations shown in Figure ED4 were repeated with altered initial allele frequencies $\square_0 \in \{0.0005, 0.01\}$, and the entire set including $\square_0 = 0.0005$, plotted as a function of the number of simulated derived alleles. The vertical line indicates the 30 derived alleles present in our aDNA dataset. *Abbreviations:* number (nb.), derived (der.)

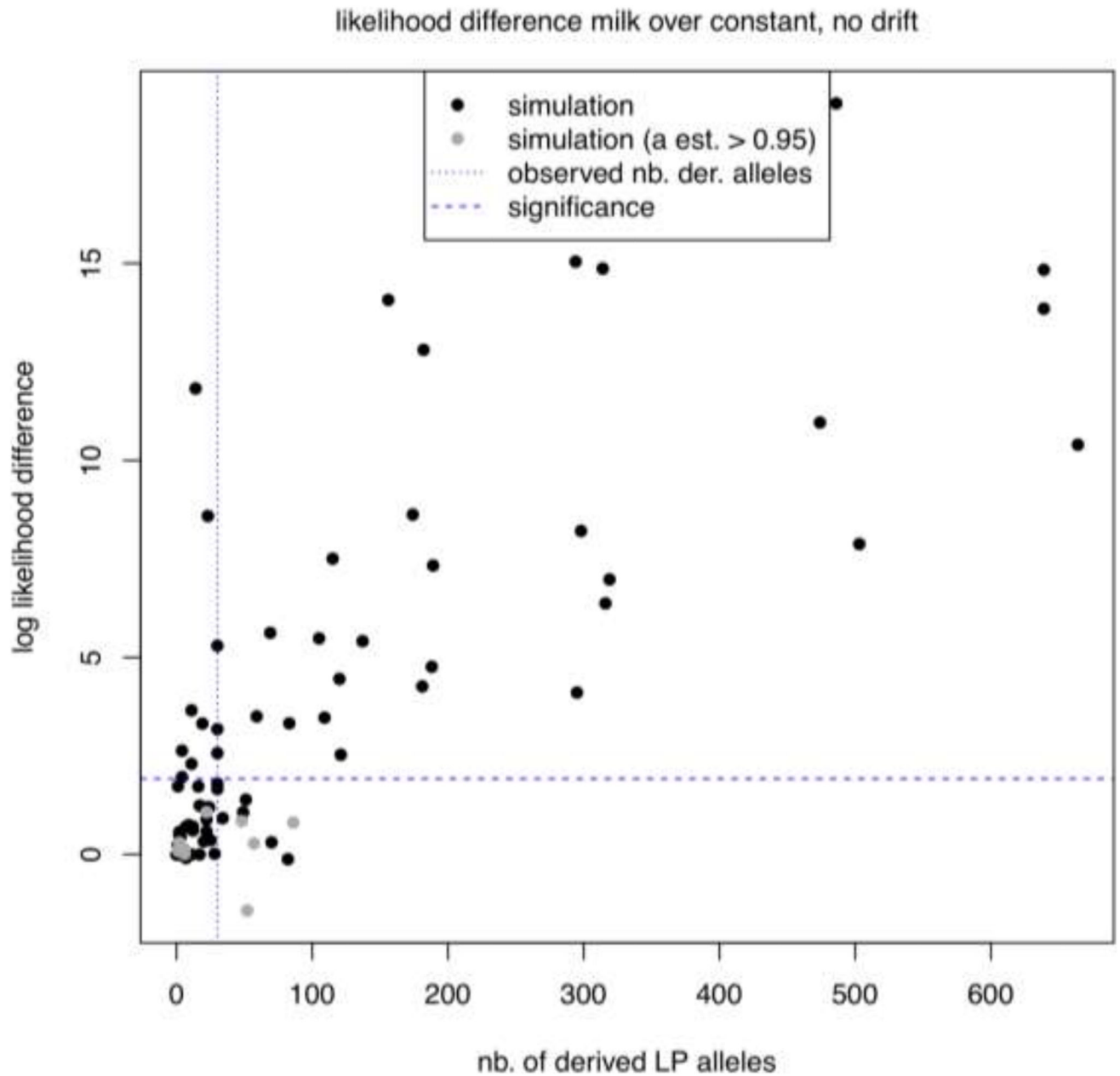


Figure ED6. Likelihood differences between constant and fluctuating selection model driven by milk exploitation in relation to the number of derived alleles simulated without drift.

Same simulations as in Figure ED5. Note that parameter optimisation on simulated data was not initialised with the parameters found for the constant model, which can lead to likelihoods of the milk model to fall below the one of the former. *Abbreviations:* number (nb.), estimate (est.), derived (der.)

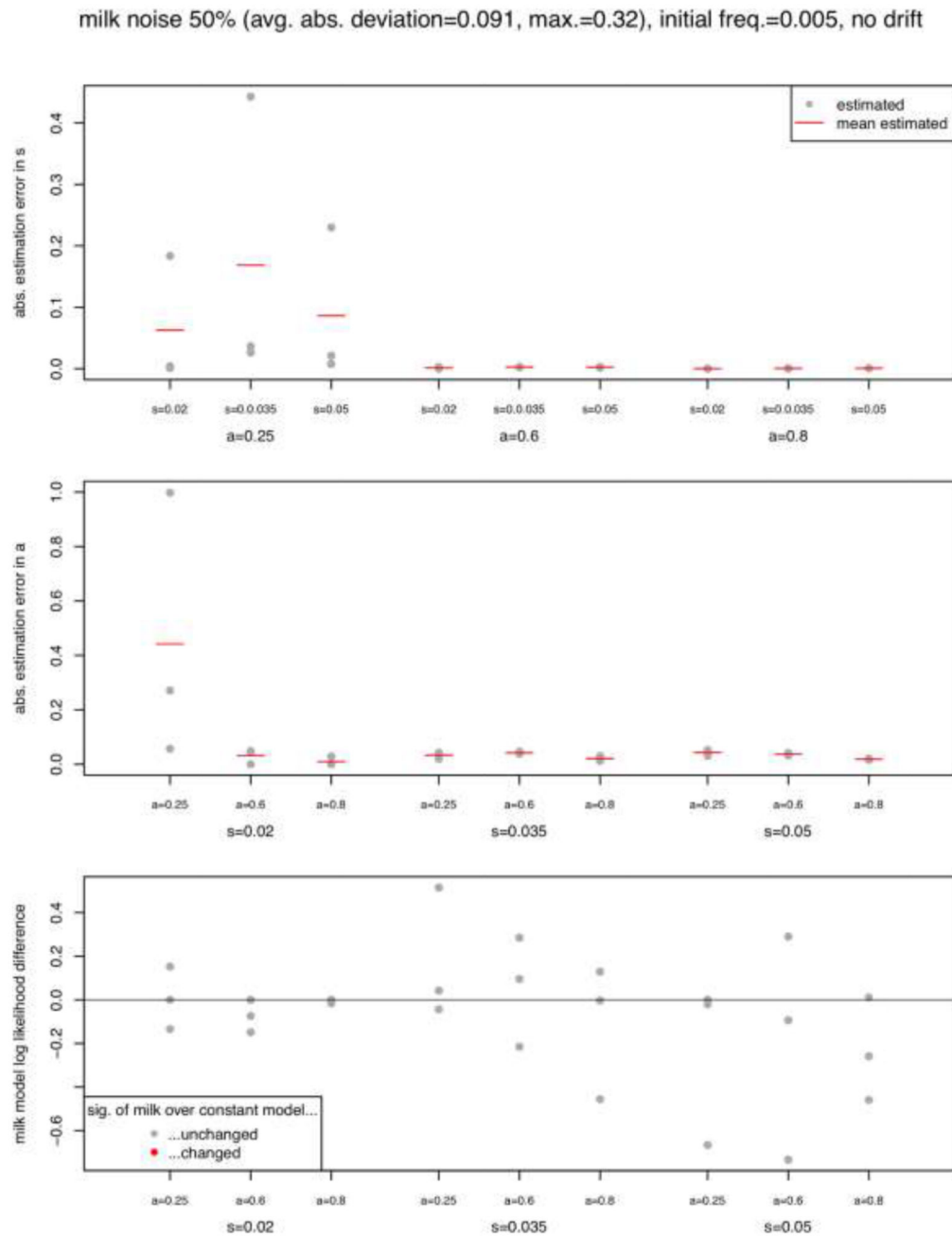
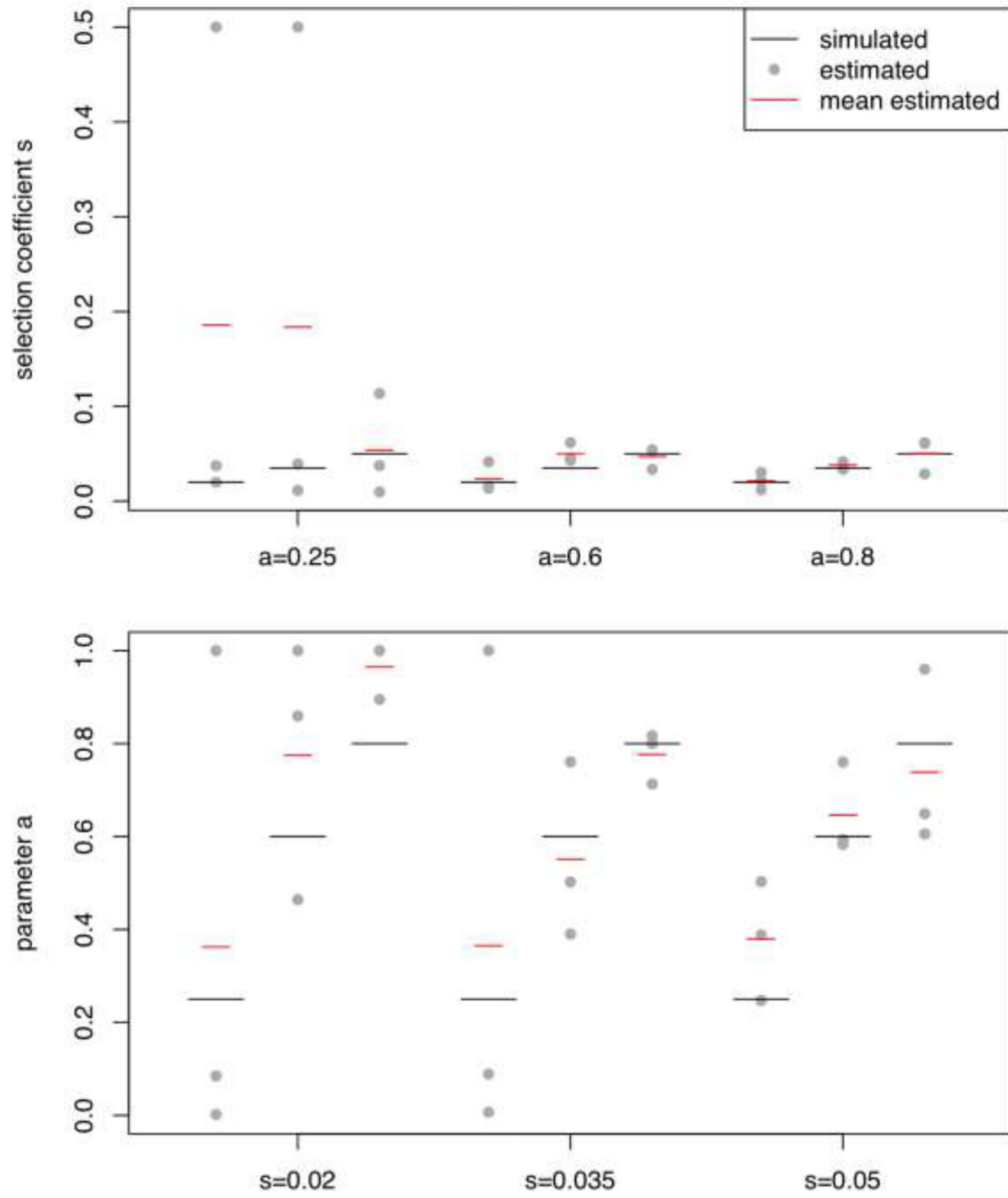


Figure ED7. Effect of noise in milk exploitation ecological proxy on parameter estimates and likelihood differences.

For each simulation presented in Figure ED4, optimisation was repeated with a noisy version of the milk exploitation variable (see Method section on aDNA analysis, subsection ‘Power analysis’ for details on how noise was simulated), and the effect on parameter estimates and likelihood differences quantified. *Abbreviations:* average (avg.), absolute (abs.), maximum (max.), frequency (freq.), significance (sig.)

initial freq.=0.005, N_e=10000



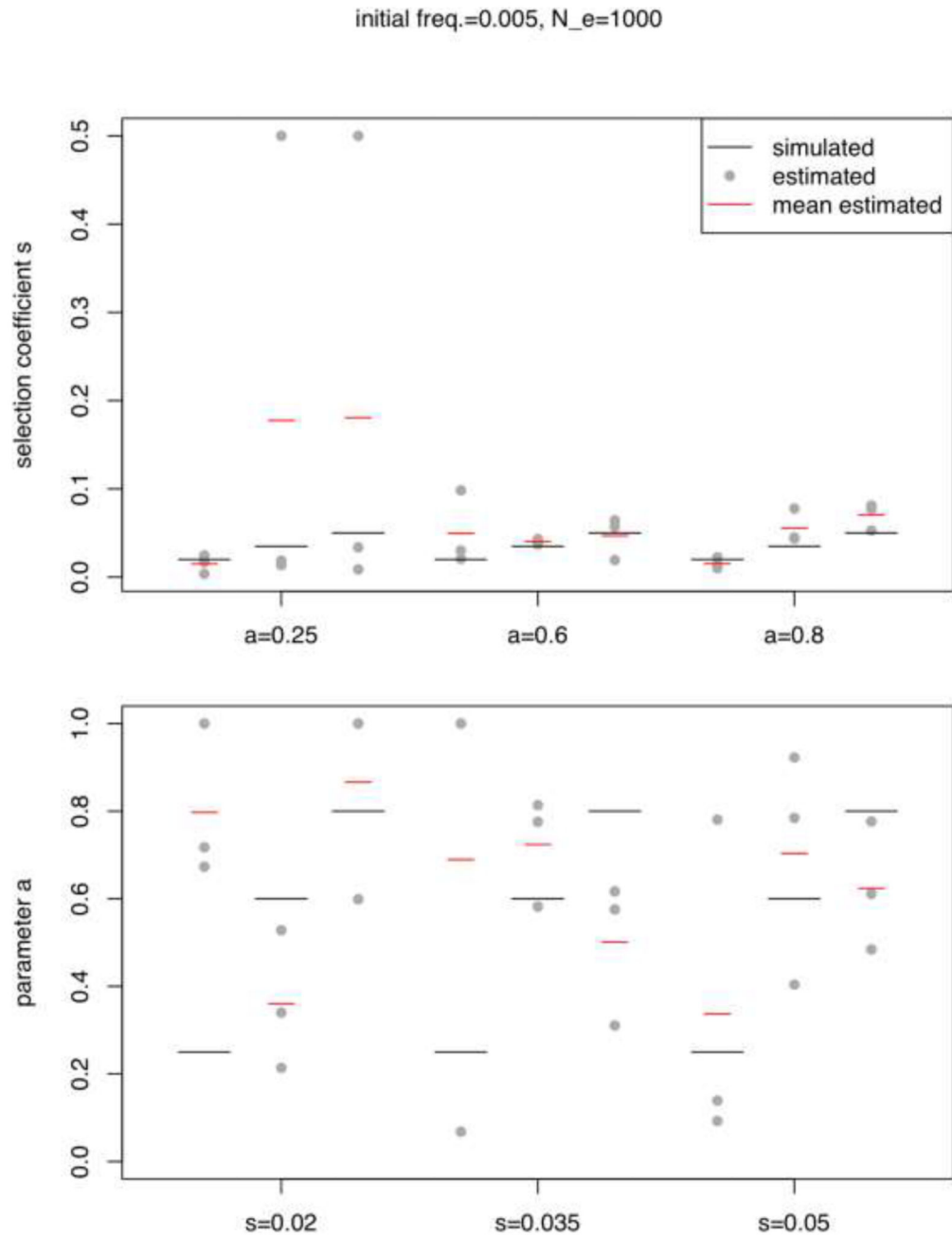
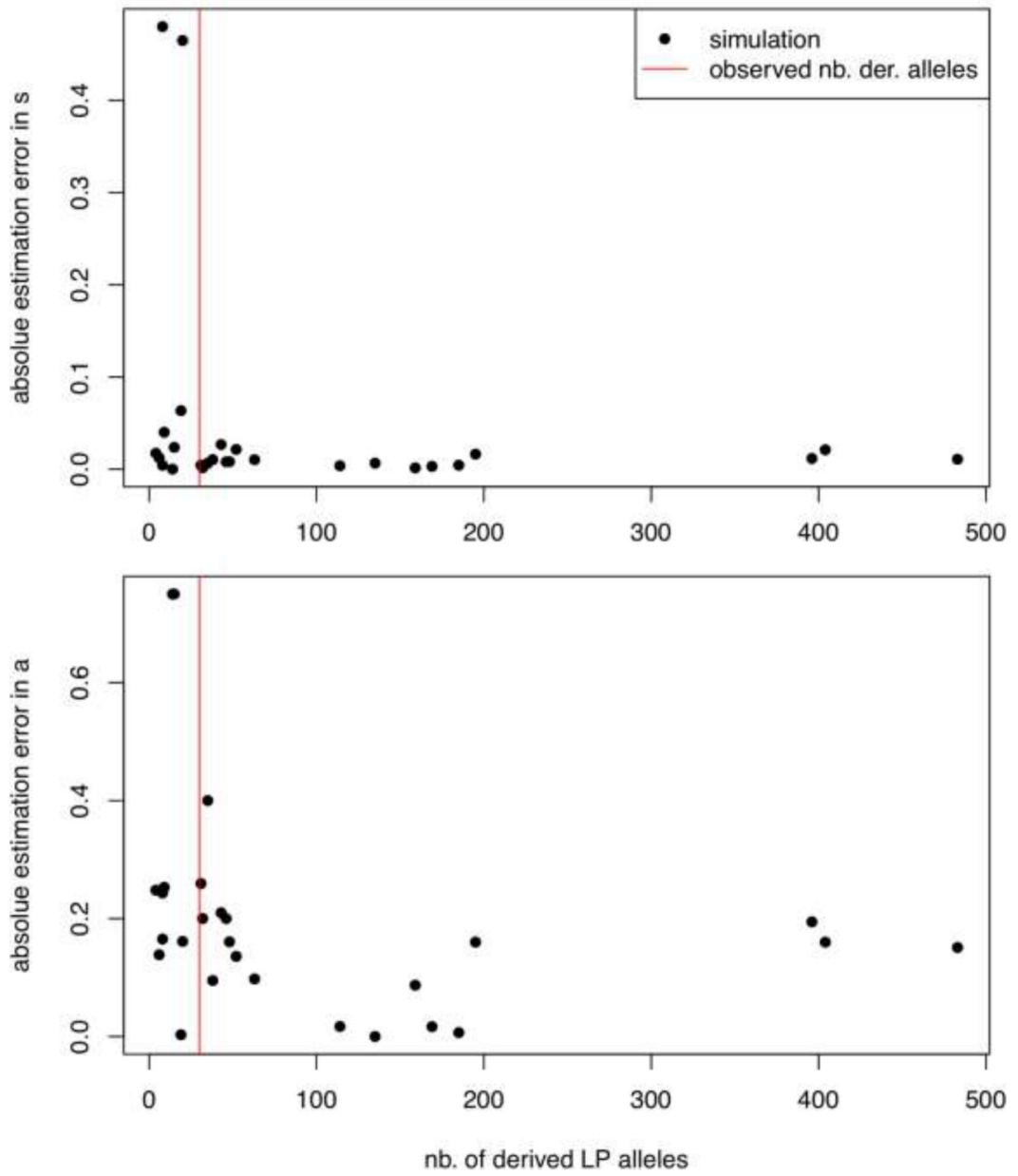


Figure ED8. A-B—Parameter estimation accuracy with drift.

Same experiment as presented in Figure ED4, but with drift at two levels ($\square \in \{1,000, 10,000\}$) affecting the simulated allele frequency trajectories. *Abbreviations:* average (avg.), absolute (abs.), frequency (freq.), significance (sig.)

$N_e = 10000$



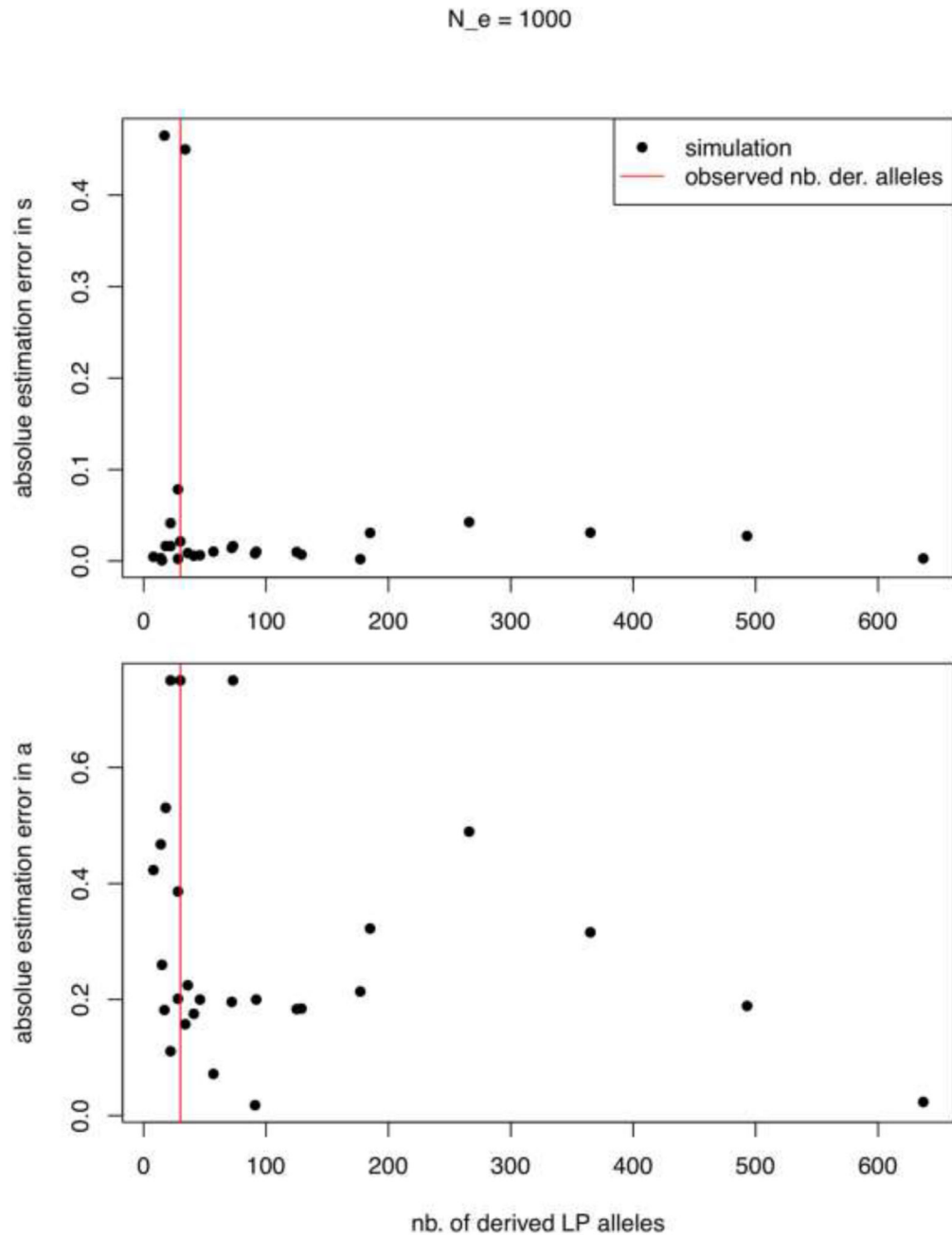
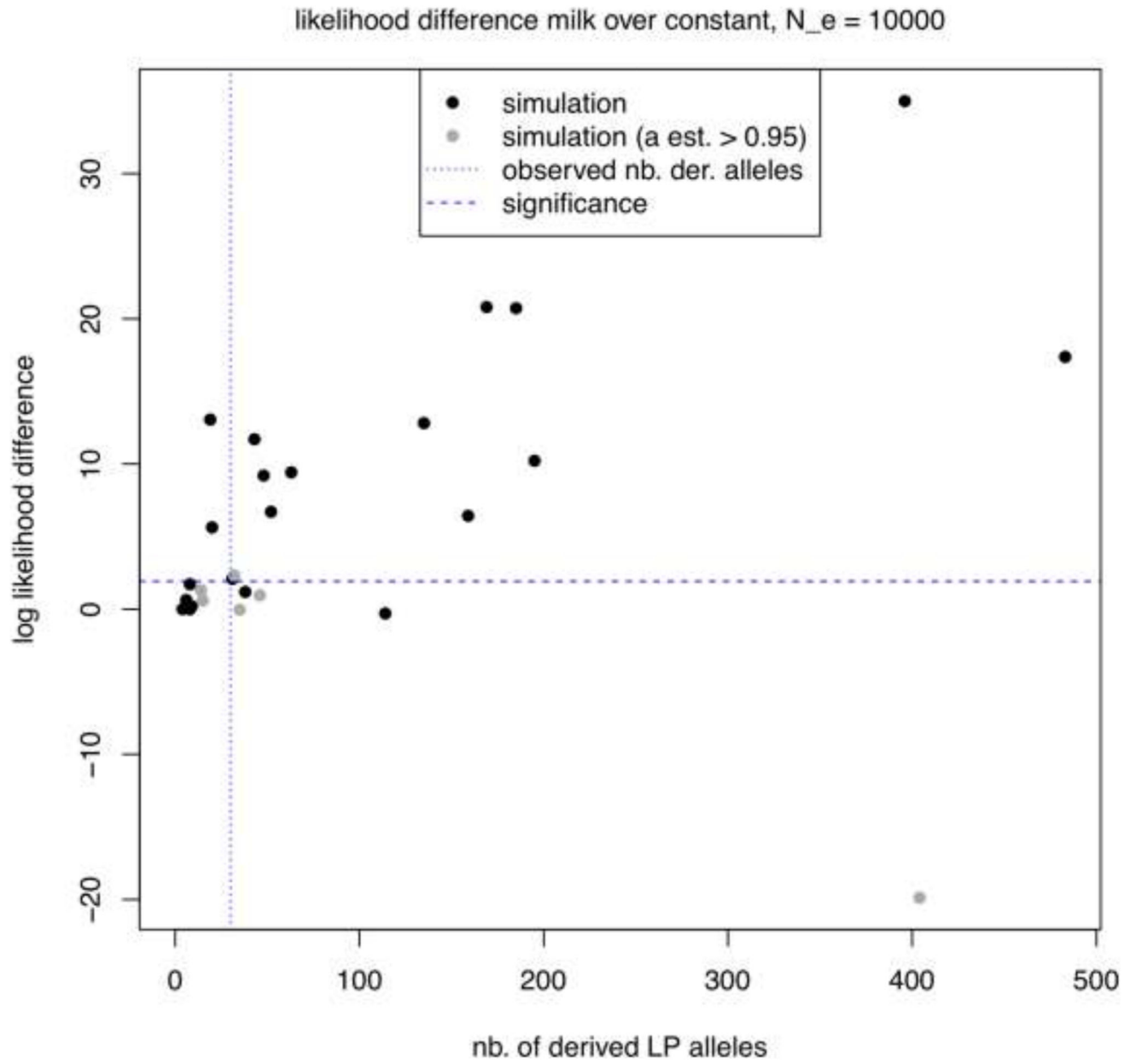


Figure ED9. A-B—Parameter estimation accuracy in relation to the number of derived alleles simulated with drift.

Replotting of data from Figure ED8 as a function of the number of simulated derived alleles.

Abbreviations: average (avg.), absolute (abs.), frequency (freq.), significance (sig.)



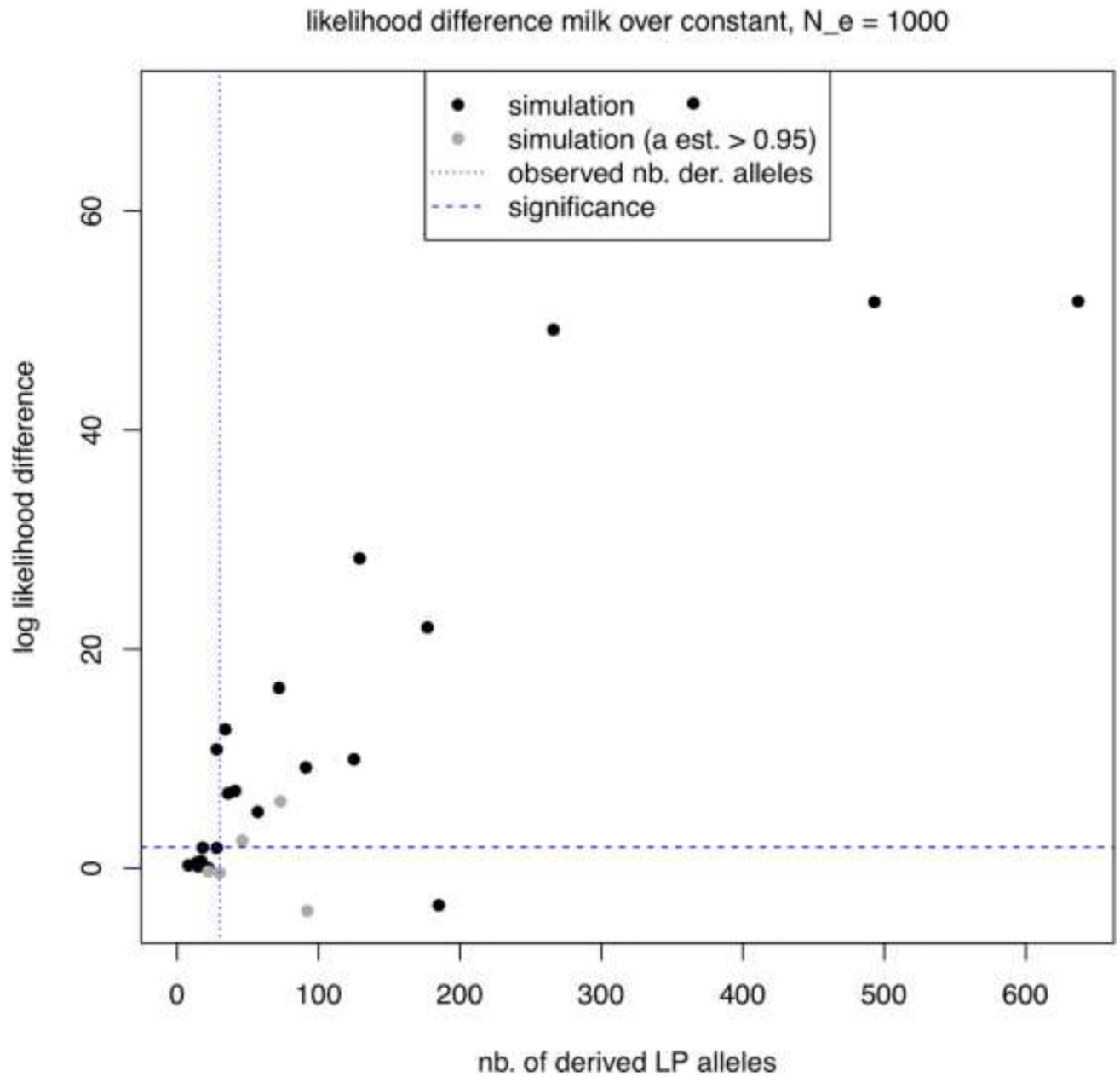


Figure ED10. A-B—Likelihood differences between constant and fluctuating selection model driven by milk exploitation in relation to the number of derived alleles simulated with drift. Same simulations as in Figure ED8 and ED9. Note that parameter optimisation on simulated data was not initialised with the parameters found for the constant model, which can lead to likelihoods of the milk model to fall below the one of the former. *Abbreviations:* average (avg.), absolute (abs.), frequency (freq.), significance (sig.)

Table ED1
Model selection results for the tested ecological time series.

Columns 5-7 show the maximum likelihood parameter estimates. The last columns list the quantities needed for multiple testing correction by control of the false discovery rate via Benjamini-Hochberg procedure. The null hypothesis of constant selection is rejected at significance level δ , here $\delta = 0.02$, in favor of a fluctuating selection model when the $\hat{\Delta}$ value of the test with rank Δ is below $\delta \frac{\Delta}{9}$ where nine is the total number of hypothesis tests.

Due to the parametrisation of fitness, the dominant selection coefficient has to be multiplied by a factor 2 to be comparable to the additive models (see Methods section on ancient DNA analysis for details). *Abbreviations:* number (nb.), parameters (par.), logarithmic (log.), likelihood ratio test (LRT), inverse (inv.), fluctuation (fluc.)

Model	nb. of par.	log. likelihood	LRT p -value	\hat{y}_0	\hat{s}	\hat{a}	rank ; δ^j	reject H_0 ?
constant, additive	2	-138.699464119656	NA	0.0013	0.022	NA	NA	NA
milk, additive	3	-138.699464119656	0.999999809769497	0.0013	0.022	1	8; 0.018	False
insolation, additive	3	-138.699464119656	1	0.0013	0.022	1	9; 0.02	False
insolation inv., additive	3	-131.702289227844	0.000183360816035128	9e-04	0.045	0.503	1; 0.002	True
population fluc., additive	3	-132.204402436158	0.000313138336841865	0.001	0.147	0.259	2; 0.004	True
population fluc. inv., additive	3	-138.699464062158	0.999729429294902	0.0013	0.022	1	7; 0.016	False
cluster, additive	3	-133.04565281483	0.000771895423444998	7e-04	0.036	0.729	3; 0.007	True
cluster inv., additive	3	-138.699464057882	0.999719547722535	0.0013	0.022	1	6; 0.013	False
domesticates, additive	3	-138.699464057103	0.99971778486365	0.0013	0.022	1	5; 0.01	False
wild, additive	3	-135.062356151726	0.00699514207820942	4e-04	0.052	0.696	4; 0.009	True
constant, dominant	2	-138.664174169131	NA	0.0012	0.011	NA	NA	NA
milk, dominant	3	-138.664174150102	0.999844347386256	0.0012	0.011	1	8; 0.018	False
insolation, dominant	3	-138.664174104147	0.999712354249303	0.0012	0.011	1	6; 0.013	False
insolation inv., dominant	3	-131.753282965012	0.000200992483171354	8e-04	0.024	0.496	1; 0.002	True
population fluc., dominant	3	-132.129289121744	0.0003000999665612	0.001	0.089	0.245	2; 0.004	True

Model	nb. of par.	log. likelihood	LRT p -value	\hat{y}_0	\hat{s}	\hat{a}	rank ; δ^j	reject H_0 ?
population fluc. inv., dominant	3	-138.664174093425	0.99968952937304	0.0012	0.011	1	5; 0.01	False
cluster, dominant	3	-133.014356965802	0.000775223542268811	7e-04	0.019	0.724	3; 0.007	True
cluster inv., dominant	3	-138.664174112268	0.999730927447785	0.0012	0.011	1	7; 0.016	False
domesticates, dominant	3	-138.664174150102	0.999844347386256	0.0012	0.011	1	9; 0.02	False
wild, dominant	3	-135.137507299365	0.00791178688664611	4e-04	0.028	0.687	4; 0.009	True

Table ED2

Lactase genotype frequency and test for departure from Hardy-Weinberg equilibrium. Lactase persistence genotype (LCT -13910) frequencies in UK Biobank (stratified by self-reported ethnic background, field 21000) and gnomAD v3 (accessed 28/02/2020) showing strong departure from Hardy-Weinberg equilibrium in European and East Asian populations. AF, allele frequency. N, sample size. AA, homozygous lactase persistent. GA, heterozygous lactase persistent. GG, homozygous lactase non-persistent. P, chi-squared test for departure from Hardy-Weinberg equilibrium. X^2 , chi-squared statistic.

Population	AF	N	AA	GA	GG	P	x^2
UK Biobank							
White, British	0.74	354998	197789	133046	24163	1.46×10^{-18}	77.31
White, Irish	0.84	10664	7533	2864	267	0.81	0.06
Any other white background	0.50	14739	4310	6121	4308	6.90×10^{-94}	422.52
White and Black Caribbean	0.51	203	44	121	38	0.01	7.01
White and Black African	0.46	98	18	54	26	0.35	0.87
White and Asian	0.51	298	69	167	62	0.04	4.04
Any other mixed background	0.47	466	94	250	122	0.11	2.53
Indian	0.58	19	7	8	4	0.79	0.07
Pakistani	0.50	7	1	5	1	0.55	0.36
Any other Asian background	0.09	171	1	29	141	0.92	0.01
Caribbean	0.95	10	9	0	1		
African	0.30	5	1	1	3	0.67	0.18
Any other Black background	0.75	4	2	2	0	-	-
Chinese	0.67	3	1	2	0	-	-
Other ethnic group	0.25	1562	199	385	978	9.76×10^{42}	183.19

Population	AF	N	AA	GA	GG	P	x ²
gnomAD							
Amish	0.76	448	267	149	32	0.10	2.68
European (non-Finnish)	0.64	32263	13797	13617	4849	3.32 x 10 ⁻⁵³	235.75
European (Finnish)	0.58	5202	1729	2543	930	0.94	0.01
Other	0.31	1074	128	408	538	3.59 x 10 ⁻⁰⁴	12.74
Latino	0.23	6820	393	2370	4057	0.06	3.50
South Asian	0.17	1521	55	393	1073	0.02	5.82
Ashkenazi Jewish	0.13	1661	23	383	1255	0.35	0.86
African	0.12	20992	340	4561	16091	0.43	0.62
East Asian	9.58 x 10 ⁻⁰⁴	1566	0	3	1563	1.57 x 10 ⁻³⁹	173.08

Table ED3

Lactase persistence genotype correlation between spousal pairs in UK Biobank. Association of individual lactase persistence genotype on spouse genotype adjusted for age, partner age, top ten genetic principal components and partner top ten genetic principal components. Sensitivity analyses were additionally adjusted for top 40 genetic principal components. Additive and dominant inheritance models were evaluated. CI, confidence interval. N, sample size. OR, odds ratio.

Test	N	Effect	95% CI	P
Additive	46,560	0.004	-0.002 0.011	0.22
Additive (sensitivity)	46,560	0.004	-0.003 0.010	0.26
Dominant	46,560	OR 1.10	1.001 1.220	0.05
Dominant (sensitivity)	46,560	OR 1.11	1.001 1.221	0.05

Table ED4

Proportion of significant likelihood differences between constant and fluctuating selection model driven by milk exploitation.

Proportions are given separately for models with parameter close to one, as these are generally indistinguishable from constant selection models, and contrast the proportions for simulations with less and at least the same number of derived alleles as observed in the real aDNA data. *Abbreviations:* frequency (freq.), estimate (est.), number (nb.), derived (der.), alleles (al.), observed (obs.)

N _e	initial freq.	est. of $\Delta < 0.95$			est. of $\Delta \geq 0.95$		
		all	nb. der. al. obs.	nb. der. al. < obs.	all	nb. der. al. obs.	nb. der. al. < obs.
NA	0.005	0.63	0.86	0.3	0.0	0.0	0.0
10,000	0.005	0.67	0.86	0.29	0.25	0.17	0.0
1,000	0.005	0.64	0.93	0.125	0.4	0.5	0.0

Authors

Richard P. Evershed¹, George Davey-Smith^{2,3,4}, Mélanie Roffet-Salque¹, Adrian Timpson^{5,6}, Yoan Diekmann^{5,7}, Matthew S. Lyon^{2,3,4}, Lucy J. E. Cramp⁸, Emmanuelle Casanova¹, Jessica Smyth^{1,9}, Helen L. Whelton¹, Julie Dunne¹, Veronika Brychova^{10,11}, Lucija Šoberl¹, Pascale Gerbault^{12,4}, Rosalind E. Gillis^{13,14}, Volker Heyd^{7,15}, Emily Johnson^{16,17}, Iain Kendall¹, Katie Manning¹⁸, Arkadiusz Marciniak¹⁹, Alan K. Outram¹⁶, Jean-Denis Vigne¹³, Stephen Shennan²⁰, Andrew Bevan²⁰, Sue Colledge²⁰, Lyndsay Allason-Jones²¹, Luc Amkreutz²², Alexandra Anders²³, Rose-Marie Arbogast²⁴, Adrian Bălăescu²⁵, Eszter Banffy^{26,27}, Alistair Barclay²⁸, Anja Behrens²⁹, Peter Bogucki³⁰, Ángel Carrancho Alonso³¹, José Miguel Carretero^{32,33}, Nigel Cavanagh³⁴, Erich Classen³⁵, Hipolito Collado Giraldo^{36,37}, Matthias Conrad³⁸, Piroska Csengeri³⁹, Lech Czerniak⁴⁰, Maciej Dębiec⁴¹, Anthony Denaire⁴², László Domboróczy⁴³, Christina Donald⁴⁴, Julia Ebert⁴⁵, Christopher Evans⁴⁶, Marta Francés-Negro³², Detlef Gronenborn⁴⁷, Fabian Haack⁴⁸, Matthias Halle³⁸, Caroline Hamon⁴⁹, Roman Hülshoff⁵⁰, Michael Ilett⁴⁹, Eneko Iriarte³², János Jakucs²⁶, Christian Jeunesse²⁴, Melanie Johnson⁵¹, Andy M. Jones⁵², Necmi Karul⁵³, Dmytro Kiosak^{54,55}, Nadezhda Kotova⁵⁶, Rudiger Krause⁵⁷, Saskia Kretschmer³⁸, Marta Krüger⁵⁸, Philippe Lefranc⁵⁹, Olivia Lelong^{60,61}, Eva Lenneis⁶², Andrey Logvin⁶³, Friedrich Lüth²⁹, Tibor Marton²⁶, Jane Marley⁶⁴, Richard Mortimer⁶⁵, Luiz Oosterbeek^{66,37,67}, Krisztián Oross²⁶, Juraj Pavúk⁶⁸, Joachim Pechtl^{69,70}, Pierre Pétrequin⁷¹, Joshua Pollard⁷², Richard Pollard⁷³, Dominic Powlesland⁷⁴, Joanna Pyzel⁴⁰, Pál Raczky²³, Andrew Richardson⁷⁵, Peter Rowe^{76,77}, Stephen Rowland⁷⁸, Ian Rowlandson⁷⁹, Thomas Saile⁸⁰, Katalin Sebők²³, Wolfram Schier⁴⁵, Geromo Schmalfuß³⁸, Svetlana Sharapova⁸¹, Helen Sharp⁷³, Alison Sheridan⁸², Irina Shevnina⁶³, Iwona Sobkowiak-Tabaka^{83,84}, Peter Stadler⁶², Harald Stauble³⁸, Astrid Stobbe⁵⁷, Darko Stojanovski^{85,86}, Nenad Tasic⁸⁷, Ivo van Wijk⁸⁸, Ivana Vostrovská^{89,90}, Jasna Vuković⁸⁷, Sabine Wolfram⁹¹, Andrea Zeeb-Lanz⁹², Mark G. Thomas^{93,5}

Affiliations

¹Organic Geochemistry Unit, School of Chemistry, University of Bristol, Bristol, UK

²MRC Integrative Epidemiology Unit, University of Bristol, Bristol, UK

³Population Health Sciences, Bristol Medical School, University of Bristol, Bristol, UK

⁴NIHR Bristol Biomedical Research Centre, University of Bristol, Bristol, UK

⁵Department of Genetics, Evolution and Environment, University College London, London, UK

⁶Present address: Max Planck Institute for the Science of Human History, Jena, Germany

⁷Palaeogenetics Group, Institute of Organismic and Molecular Evolution (iomE), Johannes Gutenberg University Mainz, Mainz, Germany

- ⁸Department of Anthropology and Archaeology, University of Bristol, Bristol, UK
- ⁹School of Archaeology, University College Dublin, Dublin, Ireland
- ¹⁰Department of Dairy, Fat and Cosmetics, University of Chemistry and Technology Prague, Prague, Czech Republic
- ¹¹Present address: Nuclear Dosimetry Department, Institute of Nuclear Physics of the Czech Academy of Sciences, Prague, Czech Republic
- ¹²School of Life Sciences, University of Westminster, London, UK
- ¹³Archéozoologie, Archéobotanique: Sociétés, Pratiques et Environnement (UMR 7209), CNRS-Muséum National d'Histoire Naturelle–Sorbonne Universités, Paris, France
- ¹⁴ICArEHB, Faculdade de Ciências Humanas e Sociais, Universidade do Algarve, Faro, Portugal
- ¹⁵Present address: Department of Cultures, Section of Archaeology, University of Helsinki, Helsinki, Finland
- ¹⁶Department of Archaeology, University of Exeter, Exeter, UK
- ¹⁷Present address: Archaeology South-East, UCL Institute of Archaeology, University College London, London, UK
- ¹⁸Department of Geography, King's College London, London, UK
- ¹⁹Institute of Prehistory, Adam Mickiewicz University, Poznań, Poland
- ²⁰UCL Institute of Archaeology, University College London, London, UK
- ²¹Great North Museum (former Museum of Antiquities), Newcastle, UK
- ²²National Museum of Antiquities, Leiden, The Netherlands
- ²³Institute of Archaeological Sciences, Eötvös Loránd University, Budapest, Hungary
- ²⁴UMR 7044, ARCHIMEDE, University of Strasbourg, Strasbourg, France
- ²⁵Department of Bioarchaeology, “Vasile Pârvan” Institute of Archaeology, Romanian Academy, Bucharest, Romania
- ²⁶Institute of Archaeology, Research Centre for the Humanities, Eötvös Loránd Research Network, Centre of Excellence of the Hungarian Academy of Sciences, Budapest, Hungary
- ²⁷Römisch-Germanische Kommission, Frankfurt am Main, Germany
- ²⁸Cotswold Archaeology, Cirencester, UK
- ²⁹German Archaeological Institute, Berlin, Germany
- ³⁰School of Engineering and Applied Science, Princeton University, Princeton, USA

- ³¹Área de Prehistoria, Departamento de Historia, Geografía y Comunicación, University of Burgos, Burgos, Spain
- ³²Laboratorio Evolución Humana, University of Burgos, Burgos, Spain
- ³³Centro Mixto UCM-ISCIII de Evolución y Comportamiento Humana, Spain
- ³⁴Network Archaeology, Lincoln, UK
- ³⁵Present address: LVR-State Service for Archaeological Heritage, Bonn, Germany
- ³⁶Patrimonio & Arte Research Group, Extremadura University, Badajoz and Cáceres, Spain
- ³⁷Geosciences Centre, Coimbra University, Coimbra, Portugal
- ³⁸Landesamt für Archäologie, Dresden, Germany
- ³⁹Herman Ottó Museum, Miskolc, Hungary
- ⁴⁰Institute of Archaeology and Ethnology, University of Gdansk, Gdansk, Poland
- ⁴¹Institute of Archaeology, University Rzeszów, Rzeszów, Poland
- ⁴²UMR 6298, ARTEHIS, University of Burgundy, Dijon, France
- ⁴³Dobó István Castle Museum, Eger, Hungary
- ⁴⁴The McManus: Dundee's Art Gallery & Museum, Dundee, UK
- ⁴⁵Institute of Prehistoric Archaeology, Free University of Berlin, Berlin, Germany
- ⁴⁶Cambridge Archaeological Unit, University of Cambridge, Cambridge, UK
- ⁴⁷Römisch-Germanisches Zentralmuseum, Leibniz Research Institute for Archaeology, Mainz, Germany
- ⁴⁸Archaeological Department, Landesmuseum Württemberg, Stuttgart, Germany
- ⁴⁹UMR 8215, Trajectoires, Université Paris 1 Panthéon-Sorbonne, Paris, France
- ⁵⁰State Office for Heritage Management and Archaeology, Saxony Anhalt/State Museum of Prehistory, Halle/Saale, Germany
- ⁵¹CFA Archaeology, Musselburgh, UK
- ⁵²Cornwall Archaeological Unit, Cornwall Council, Truro, UK
- ⁵³Istanbul University, Istanbul, Turkey
- ⁵⁴"I.I. Mechnikov", Odessa National University, Odessa, Ukraine
- ⁵⁵Ca' Foscari, University of Venice, Venice, Italy
- ⁵⁶Institute of Archaeology of Academy of Science of Ukraine, Kiev, Ukraine
- ⁵⁷Prehistory Department, Institut of Archaeology, Johann Wolfgang Goethe-Universität, Frankfurt am Main, Germany
- ⁵⁸Department of Archaeology, Adam Mickiewicz University, Poznan, Poland

- ⁵⁹UMR 7044, INRAP Grand-Est Sud, University of Strasbourg, Strasbourg, France
- ⁶⁰GUARD Glasgow, Glasgow, UK
- ⁶¹Present address: University of West England, Bristol, UK
- ⁶²Department of Prehistoric and Historical Archaeology, University of Vienna, Vienna, Austria
- ⁶³Kostanay State University, Kostanay, Kazakhstan
- ⁶⁴Royal Cornwall Museum, Truro, UK
- ⁶⁵Oxford Archaeology East, Oxford, UK
- ⁶⁶Polytechnic Institute of Tomar, Tomar, Portugal
- ⁶⁷Terra e Memória Institute, Mação, Portugal
- ⁶⁸Archeologický ústav SAV, Nitra, Slovakia
- ⁶⁹Kelten Römer Museum Manching, Manching, Germany
- ⁷⁰Present address: Department of Archaeology, University of Innsbruck, Innsbruck, Austria
- ⁷¹MSHE C.N. Ledoux, CNRS & University of Franche-Comté, Besancon, France
- ⁷²Department of Archaeology, University of Southampton, Southampton, UK
- ⁷³Leicestershire County Council Museums, Leicestershire, UK
- ⁷⁴The Landscape Research Centre Ltd., West Heslerton, UK
- ⁷⁵Canterbury Archaeological Trust, Canterbury, UK
- ⁷⁶Tees Archaeology, Hartlepool, UK
- ⁷⁷Present address: North Yorkshire County Council HER, Northallerton, UK
- ⁷⁸Oxford Archaeology North, Lancaster, UK
- ⁷⁹Archaeological Consultancy, Emsworth, UK
- ⁸⁰Institute of History, University of Regensburg, Regensburg, Germany
- ⁸¹Institute of History and Archaeology, UB RAS, Ekaterinburg, Russia
- ⁸²National Museums Scotland, Edinburgh, UK
- ⁸³Institute of Archaeology and Ethnology, Polish Academy of Sciences, Poznan, Poland
- ⁸⁴Present address: Faculty of Archaeology, Adam Mickiewicz University, Poznan, Poland
- ⁸⁵Geology Department, University of Trás-os-Montes and Alto Douro, Vila Real, Portugal
- ⁸⁶Department of Humanistic Studies, University of Ferrara, Ferrara, Italy

⁸⁷University of Belgrade, Belgrad, Serbia

⁸⁸Faculty of Archaeology, Leiden University, Leiden, The Netherlands

⁸⁹Institute of Archaeology and Museology, Masaryk University, Brno, Czech Republic

⁹⁰Present address: Department of History, Palackv University, Olomouc, Czech Republic

⁹¹Staatliches Museum für Archäologie, Chemnitz, Germany

⁹²Generaldirektion Kulturelles Erbe Rheinland-Pfalz, Dir. Landesarchäologie, Speyer, Germany

⁹³UCL Genetics Institute, University College London, London, UK

Acknowledgements

This study was funded by the European Research Council Advanced Grant —NeoMilk” FP7-IDEAS- ERC/ 324202. MR-S thanks the Royal Society for funding her Dorothy Hodgkin Fellowship (DHF\R1\180064 and RGF\EA\181067). NERC (Reference: CC010) and NEIF (www.isotopesuk.org) are thanked for funding and maintenance of the GC-MS and GC-C-IRMS instruments used for this work. GDS and MSL work in the MRC Integrative Epidemiology Unit at the University of Bristol (MC_UU_00011/1). Dr Penny Bickle (University of York, UK) and Mr David Altoft are acknowledged for the sampling of some potsherds from this study. We thank Saule Kalieva and Victor Logvin (Kostanay State University, Kazakhstan), Christian Lohr (Leibniz Research Institute for Archaeology, Mainz, Germany), Jens Lüning (Johann Wolfgang Goethe-Universität, Frankfurt am Main, Germany), Ivan Pavl (Institute of Archaeology of the Academy of Sciences of the Czech Republic), and Ralf W. Schmitz (LVR-LandesMuseum, Bonn, Germany) for providing some of the sherds presented in this study. We are grateful to Dr Karen Dwyer, teaching fellow in English grammar and research methodology at UCL, for clarifying *lactase non-persistence* as the correct usage over *non-lactase persistence*, on the basis that *non* qualifies *persistence*, even if *lactase persistence* is considered a compound noun. We are also grateful to Dr Laurence Howe, Senior Research Associate at the MRC IEU for providing derived spousal pairs in UK Biobank. The authors acknowledge the use of the UCL Computer Science ECON High-Performance Computing (HPC) Cluster (ECON@UCL), and associated support services, in the completion of this work. This study was supported by the NIHR Biomedical Research Centre at University Hospitals Bristol and Weston NHS Foundation Trust and the University of Bristol. The views expressed are those of the author(s) and not necessarily those of the NIHR or the Department of Health and Social Care.

Data availability statement

Data for running the ancient DNA analyses are available from: <https://github.com/ydiekmann/Evershed> Nature 2022 KML files, a summary of archaeological milk residue data, ecological proxy variables, and a summary of radiocarbon dates are available from: <https://github.com/AdrianTimpson/2020-03-03523A>

UK Biobank data are available from <https://www.ukbiobank.ac.uk/>

Code availability statement

R and Python code for running the ancient DNA analyses are available from: https://github.com/ydiekmann/Evershed_Nature_2022

Open-source R Code for running the UK Biobank analyses under MIT license are available from: <https://github.com/MRCIEU/lp-coevolution>

R Code for the generation of Figs 1,2,3 and methods Figs 1 and 2; polygon are available from: <https://github.com/AdrianTimpson/2020-03-03523A>

References

1. Sabeti PC, et al. Positive natural selection in the human lineage. *Science*. 2006; 312: 1614. [PubMed: 16778047]
2. Evershed RP, et al. Earliest date for milk use in the Near East and southeastern Europe linked to cattle herding. *Nature*. 2008; 455: 528–531. [PubMed: 18690215]
3. Debono Spiteri C, et al. Regional asynchronicity in dairy production and processing in early farming communities of the northern Mediterranean. *Proc Natl Acad Sci USA*. 2016; 113: 13594–13599. [PubMed: 27849595]
4. Collins R. What makes UK Biobank special? *Lancet*. 2012; 379: 1173–1174. [PubMed: 22463865]
5. Allen NE, Sudlow C, Peakman T, Collins R. UK Biobank Data: Come and Get It. *Sci Transl Med*. 2014; 6 224ed224
6. Gerbault P, et al. Evolution of lactase persistence: an example of human niche construction. *Philos Trans R Soc Lond, B, Biol Sci*. 2011; 366: 863–877. [PubMed: 21320900]
7. Food and Agriculture Organization of the United Nations (FAO). FAOSTAT. Available at <http://www.fao.org/faostat/en/#data/QA>
8. Vigne J-D, Helmer D. Was milk a “secondary product” in the Old World Neolithisation process? Its role in the domestication of cattle, sheep and goats. *Anthropozoologica*. 2007; 42: 9–40.
9. Roffet-Salque, M, Gillis, R, Evershed, RP, Vigne, J-D. Hybrid communities: biosocial approaches to domestication and other trans-species relationships. Stépanoff, Charles; Vigne, Jean-Denis, editors. Routledge; 2018. 127–143.
10. Gillis R, et al. Sophisticated cattle dairy husbandry at Bordusani-Popin (Romania, fifth millennium BC): the evidence from complementary analysis of mortality profiles and stable isotopes. *World Archaeol*. 2013; 45: 447–472.
11. Ethier J, et al. Earliest expansion of animal husbandry beyond the Mediterranean zone in the sixth millennium BC. *Sci Rep*. 2017; 7 7146 [PubMed: 28769118]
12. Salque M, et al. Earliest evidence for cheese making in the sixth millennium BC in northern Europe. *Nature*. 2013; 493: 522–525. [PubMed: 23235824]
13. Gillis RE, et al. The evolution of dual meat and milk cattle husbandry in Linearbandkeramik societies. *Proc Royal Soc B*. 2017; 284
14. Balasse M, Tresset A. Early weaning of Neolithic domestic cattle (Bercy, France) revealed by intra-tooth variation in nitrogen isotope ratios. *J Archaeol Sci*. 2002; 29: 853–859.
15. Casanova E, et al. Dating the emergence of dairying by the first farmers of Central Europe using ¹⁴C analysis of fatty acids preserved in pottery vessels. *Proc Natl Acad Sci USA*.
16. Whelton HL, Roffet-Salque M, Kotsakis K, Urem-Kotsou D, Evershed RP. Strong bias towards carcass product processing at Neolithic settlements in northern Greece revealed through absorbed lipid residues of archaeological pottery. *Quat Int*. 2018; 496: 127–139.
17. Copley MS, et al. Direct chemical evidence for widespread dairying in prehistoric Britain. *Proc Natl Acad Sci USA*. 2003; 100: 1524–1529. [PubMed: 12574520]
18. Cramp LJE, et al. Immediate replacement of fishing with dairying by the earliest farmers of the northeast Atlantic archipelagos. *Proc Royal Soc B*. 2014; 281 20132372
19. Smyth J, Evershed RP. Milking the megafauna: Using organic residue analysis to understand early farming practice. *Environ Archaeol*. 2016; 21: 214–229.
20. Charlton S, et al. New insights into Neolithic milk consumption through proteomic analysis of dental calculus. *Archaeol Anthropol Sci*. 2019; 11: 6183–6196.
21. Craig OE, et al. Ancient lipids reveal continuity in culinary practices across the transition to agriculture in Northern Europe. *Proc Natl Acad Sci USA*. 2011; 108: 17910–17915. [PubMed: 22025697]
22. Cramp LJE, et al. Neolithic dairy farming at the extreme of agriculture in Northern Europe. *Proc Royal Soc B*. 2014; 281 20140819

23. Pääkkonen M, Holmqvist E, Bläuer A, Evershed RP, Asplund H. Diverse economic patterns in the North Baltic Sea region in the Late Neolithic and Early Metal periods. *Eur J Archaeol.* 2019; 23: 4–21.
24. Burger J, Kirchner M, Bramanti B, Haak W, Thomas MG. Absence of the lactase-persistence-associated allele in early Neolithic Europeans. *Proc Natl Acad Sci USA.* 2007; 104: 3736–3741. [PubMed: 17360422]
25. Sverrisdóttir OÓ, et al. Direct estimates of natural selection in Iberia indicate calcium absorption was not the only driver of lactase persistence in Europe. *Mol Biol Evol.* 2014; 31: 975–983. [PubMed: 24448642]
26. Allentoft ME, et al. Population genomics of Bronze Age Eurasia. *Nature.* 2015; 522: 167–172. [PubMed: 26062507]
27. Haak W, et al. Massive migration from the steppe was a source for Indo-European languages in Europe. *Nature.* 2015; 522: 207–211. [PubMed: 25731166]
28. Brace S, et al. Ancient genomes indicate population replacement in Early Neolithic Britain. *Nat Ecol Evol.* 2019; 3: 765–771. [PubMed: 30988490]
29. Burger J, et al. Low Prevalence of Lactase Persistence in Bronze Age Europe Indicates Ongoing Strong Selection over the Last 3,000 Years. *Curr Biol.* 2020; 30: 4307–4315. e4313 [PubMed: 32888485]
30. Itan Y, Powell A, Beaumont MA, Burger J, Thomas MG. The origins of lactase persistence in Europe. *PLoS Comput Biol.* 2009; 5 e1000491 [PubMed: 19714206]
31. Enattah NS, et al. Identification of a variant associated with adult-type hypolactasia. *Nat Genet.* 2002; 30: 233–237. [PubMed: 11788828]
32. Itan Y, Jones B, Ingram C, Swallow D, Thomas M. A worldwide correlation of lactase persistence phenotype and genotypes. *BMC Evol Biol.* 2010; 10: 36. [PubMed: 20144208]
33. Flatz G, Rothauwe H. Lactose nutrition and natural selection. *Lancet.* 1973; 302: 76–77.
34. Cubas M, et al. Latitudinal gradient in dairy production with the introduction of farming in Atlantic Europe. *Nat Commun.* 2020; 11: 1–9. [PubMed: 31911652]
35. Klopstein S, Currat M, Excoffier L. The fate of mutations surfing on the wave of a range expansion. *Mol Biol Evol.* 2006; 23: 482–490. [PubMed: 16280540]
36. Gerbault P, Moret C, Currat M, Sanchez-Mazas A. Impact of selection and demography on the diffusion of lactase persistence. *PLoS One.* 2009; 4 e6369 [PubMed: 19629189]
37. Cook GC, al-Torki MT. High intestinal lactase concentrations in adult Arabs in Saudi Arabia. *Br Med J.* 1975; 3: 135–136. [PubMed: 1170003]
38. Davey Smith G, et al. Lactase persistence-related genetic variant: population substructure and health outcomes. *Eur J Hum Genet.* 2009; 17: 357–367. [PubMed: 18797476]
39. Cederlund A, et al. Lactose in human breast milk an inducer of innate immunity with implications for a role in intestinal homeostasis. *PLoS One.* 2013; 8
40. Gibson PR. History of the low FODMAP diet. *J Gastroenterol Hepatol.* 2017; 32: 5–7. [PubMed: 28244673]
41. Walker, C, Thomas, MG. Lactose - Evolutionary role, health effects, and applications. Paques, Marcel; Lindner, Cordula, editors. Elsevier; 2019. 1–48. 1
42. Simoons F. Primary adult lactose intolerance and the milking habit: a problem in biologic and cultural interrelations - II. A culture historical hypothesis. *Dig Dis Sci.* 1970; 15: 695–710.
43. McCracken RD. Lactase deficiency: an example of dietary evolution. *Curr Anthropol.* 1971; 12: 479–517.
44. Holden C, Mace R. Phylogenetic analysis of the evolution of lactose digestion in adults. *Hum Biol.* 1997; 69: 605–628. [PubMed: 9299882]
45. Ingram CJE, et al. A novel polymorphism associated with lactose tolerance in Africa: multiple causes for lactase persistence? *Hum Genet.* 2007; 120: 779–788. [PubMed: 17120047]
46. Tishkoff SA, et al. Convergent adaptation of human lactase persistence in Africa and Europe. *Nat Genet.* 2007; 39: 31–40. [PubMed: 17159977]
47. Joslin SEK, et al. Association of the Lactase Persistence Haplotype Block With Disease Risk in Populations of European Descent. *Front Genet.* 2020; 11: 1346.

48. Dudd SN, Evershed RP. Direct demonstration of milk as an element of archaeological economies. *Science*. 1998; 282: 1478–1481. [PubMed: 9822376]
49. Dunne J, et al. First dairying in green Saharan Africa in the fifth millennium BC. *Nature*. 2012; 486: 390–394. [PubMed: 22722200]
50. Manning K, et al. The origins and spread of stock-keeping: the role of cultural and environmental influences on early Neolithic animal exploitation in Europe. *Antiquity*. 2013; 87: 1046–1059.
51. Shennan S, et al. Regional population collapse followed initial agriculture booms in mid-Holocene Europe. *Nat Commun*. 2013; 4 2486 [PubMed: 24084891]
52. Howe LJ, et al. Genetic evidence for assortative mating on alcohol consumption in the UK Biobank. *Nat Commun*. 2019; 10 5039 [PubMed: 31745073]
53. Rodriguez S, Gaunt TR, Day INM. Hardy-Weinberg equilibrium testing of biological ascertainment for Mendelian randomization studies. *Am J Epidemiol*. 2009; 169: 505–514. [PubMed: 19126586]
54. Mendelian Randomization of Dairy Consumption Working Group. Dairy Consumption and Body Mass Index Among Adults: Mendelian Randomization Analysis of 184802 Individuals from 25 Studies. *Clin Chem*. 2018; 64: 183–191. [PubMed: 29187356]
55. Simmons, JS, Whayne, TF, Anderson, GW, Horack, HM. *Global epidemiology A geography of disease and sanitation*. Vol. 1. William Heineman; 1944.
56. Bai Z, et al. Global environmental costs of China's thirst for milk. *Glob Change Biol*. 2018; 24: 2198–2211.
57. Simoons F. Primary adult lactose intolerance and the milking habit: a problem in biological and cultural interrelations - I. Review of the medical research. *Dig Dis Sci*. 1969; 14: 819–836.
58. Bayless TM, Paige DM, Ferry GD. Lactose intolerance and milk drinking habits. *Gastroenterology*. 1971; 60: 605–608. [PubMed: 5108166]
59. Szilagy, A, Walker, C, Thomas, MG. *Lactose: Evolutionary role, health effects, and applications*. Paques, Marcel; Lindner, Cordula, editors. Elsevier; 2019. 113–153.
60. Almon R, Álvarez-Leon EE, Serra-Majem L. Association of the European lactase persistence variant (LCT-13910 C>T polymorphism) with obesity in the Canary Islands. *PLoS One*. 2012; 7 e43978 [PubMed: 22937140]
61. Hartwig FP, Horta BL, Smith GD, de Mola CL, Victora CG. Association of lactase persistence genotype with milk consumption, obesity and blood pressure: a Mendelian randomization study in the 1982 Pelotas (Brazil) Birth Cohort, with a systematic review and meta-analysis. *Int J Epidemiol*. 2016; 45: 1573–1587. [PubMed: 27170764]
62. Qin L-Q, He K, Xu J-Y. Milk consumption and circulating insulin-like growth factor-I level: a systematic literature review. *Int J Food Sci Nutr*. 2009; 60: 330–340. [PubMed: 19746296]
63. Wiley A. The evolution of lactase persistence: milk consumption, insulin-like growth factor I, and human life-history parameters. *Q Rev Biol*. 2018; 93: 319–345.
64. Campbell CD, et al. Demonstrating stratification in a European American population. *Nat Genet*. 2005; 37: 868–872. [PubMed: 16041375]
65. Bergholdt HKM, Nordestgaard BG, Varbo A, Ellervik C. Milk intake is not associated with ischaemic heart disease in observational or Mendelian randomization analyses in 98 529 Danish adults. *Int J Epidemiol*. 2015; 44: 587–603. [PubMed: 26085675]
66. Bocquet-Appel J-P. When the world's population took off: the springboard of the Neolithic demographic transition. *Science*. 2011; 333: 560–561. [PubMed: 21798934]
67. Loog L, et al. Estimating mobility using sparse data: Application to human genetic variation. *Proc Natl Acad Sci USA*. 2017; 114: 12213–12218. [PubMed: 29087301]
68. Vorou R, Papavassiliou V, Tsiodras S. Emerging zoonoses and vector-borne infections affecting humans in Europe. *Epidemiol Infect*. 2007; 135: 1231–1247. [PubMed: 17445320]
69. Allen T, et al. Global hotspots and correlates of emerging zoonotic diseases. *Nat Commun*. 2017; 8 1124 [PubMed: 29066781]
70. Rice AL, Sacco L, Hyder A, Black RE. Malnutrition as an underlying cause of childhood deaths associated with infectious diseases in developing countries. *Bull World Health Organ*. 2000; 78: 1207–1221. [PubMed: 11100616]

71. Colledge S, Conolly J, Crema E, Shennan S. Neolithic population crash in northwest Europe associated with agricultural crisis. *Quat Res.* 2019. 1–22.
72. Manning K. The Cultural Evolution of Neolithic Europe. EUROEVOL Dataset 2: Zooarchaeological data. *JOAD.* 2016; 5
73. Chessa B, et al. Revealing the history of sheep domestication using retrovirus integrations. *Science.* 2009; 324: 532. [PubMed: 19390051]
74. Karesh WB, Cook RA, Bennett EL, Newcomb J. Wildlife trade and global disease emergence. *Emerg Infect Dis.* 2005; 11: 1000. [PubMed: 16022772]
75. Chomel BB, Belotto A, Meslin F-X. Wildlife, exotic pets, and emerging zoonoses. *Emerg Infect Dis.* 2007; 13: 6. [PubMed: 17370509]
76. Schibler J, Jacomet S, Hüster-Plogmann H, Brombacher C. Economic crash in the 37th and 36th centuries cal. BC in Neolithic lake shore sites in Switzerland. *Anthropozoologica.* 1997; 25: 553–570.
77. He Y, Yang X, Xia J, Zhao L, Yang Y. Consumption of meat and dairy products in China: a review. *Proc Nutr Soc.* 2016; 75: 385–391. [PubMed: 27334652]
78. Mak, VSW. Milk craze Body, science, and hope in China. University of Hawai'i Press; 2021.
79. Goodrich, JuliaK; , et al. Genetic Determinants of the Gut Microbiome in UK Twins. *Cell Host Microbe.* 2016; 19: 731–743. [PubMed: 27173935]
80. Paine, RR, Boldsen, JL. The evolution of human life history School for Advanced Research Advanced Seminar Series. Hawkes, K, Paine, RR, editors. School of American Research Press; 2006. 307–330.
81. Stackhouse, PW, , Jr, et al. POWER release 8 (with GIS applications) methodology (data parameters, sources, & validation) documentation date may 1, 2018 (all previous versions are obsolete)(data version 8.0. 1). NASA; 2018. Retrieved from <https://power.larc.nasa.gov>
82. Lieberman M, Lieberman D. Lactase Deficiency: A Genetic Mechanism which Regulates the Time of Weaning. *Am Nat.* 1978; 112: 625–627.
83. Ingold, T. Hunters, pastoralists and ranchers: reindeer economies and their transformations. Cambridge University Press; Cambridge: 1980.
84. Outram AK, et al. The earliest horse harnessing and milking. *Science.* 2009; 323: 1332–1335. [PubMed: 19265018]
1. Breu A, Gómez-Bach A, Heron C, Rosell-Melé A, Molist M. Variation in pottery use across the Early Neolithic in the Barcelona plain. *Archaeol Anthropol Sci.* 2021; 13: 53.
2. Brychova V, et al. Animal exploitation and pottery use during the early LBK phases of the Neolithic site of Bylany (Czech Republic) tracked through lipid residue analysis. *Quat Int.* 2021; 574: 91–101.
3. Carrer F, et al. Chemical analysis of pottery demonstrates Prehistoric origin for high-altitude alpine dairying. *PloS One.* 2016; 11 e0151442 [PubMed: 27100391]
4. Casanova E, et al. Spatial and temporal disparities in human subsistence in the Neolithic Rhineland gateway. *J Archaeol Sci.* 2020; 122 105215
5. Colonese AC, et al. The identification of poultry processing in archaeological ceramic vessels using in-situ isotope references for organic residue analysis. *J Archaeol Sci.* 2017; 78: 179–192.
6. Copley MS, et al. Direct chemical evidence for widespread dairying in prehistoric Britain. *Proc Natl Acad Sci USA.* 2003; 100: 1524–1529. [PubMed: 12574520]
7. Copley MS, et al. Dairying in antiquity. I. Evidence from absorbed lipid residues dating to the British Iron Age. *J Archaeol Sci.* 2005; 32: 485–503.
8. Copley MS, Berstan R, Straker V, Payne S, Evershed RP. Dairying in antiquity. II. Evidence from absorbed lipid residues dating to the British Bronze Age. *J Archaeol Sci.* 2005; 32: 505–521.
9. Copley MS, et al. Dairying in antiquity. III. Evidence from absorbed lipid residues dating to the British Neolithic. *J Archaeol Sci.* 2005; 32: 523–546.
10. Copley, MS, Evershed, RP. Building memories: the Neolithic Cotswold long barrow at Ascott-under-Wychwood, Oxfordshire Cardiff Studies in Archaeology. Benson, Don; Whittle, A, editors. Oxbow Books; 2006.
11. Courel B, et al. Organic residue analysis shows sub-regional patterns in the use of pottery by Northern European hunter-gatherers. *R Soc Open Sci.* 2020; 7 192016 [PubMed: 32431883]

12. Craig OE, et al. Did the first farmers of central and eastern Europe produce dairy foods? *Antiquity*. 2005; 79: 882–894.
13. Craig OE, Taylor G, Mulville J, Collins MJ, Parker Pearson M. The identification of prehistoric dairying activities in the Western Isles of Scotland: an integrated biomolecular approach. *J Archaeol Sci*. 2005; 32: 91–103.
14. Craig OE, et al. Molecular and isotopic demonstration of the processing of aquatic products in Northern European Prehistoric pottery. *Archaeometry*. 2007; 49: 135–152.
15. Craig, O. Archaeology meets science - Biomolecular investigations in Bronze Age Greece. Tzedakis, Yannis; Martlew, Holley; Jones, Martin K, editors. Oxbow Books; 2008. 121–124.
16. Craig OE, et al. Ancient lipids reveal continuity in culinary practices across the transition to agriculture in Northern Europe. *Proc Natl Acad Sci USA*. 2011; 108: 17910–17915. [PubMed: 22025697]
17. Craig OE, et al. Feeding Stonehenge: cuisine and consumption at the Late Neolithic site of Durrington Walls. *Antiquity*. 2015; 89: 1096–1109.
18. Craig-Atkins E, et al. The dietary impact of the Norman Conquest: A multiproxy archaeological investigation of Oxford, UK. *PLoS One*. 2020; 15 e0235005 [PubMed: 32628680]
19. Cramp LJE, Evershed RP, Eckardt H. What was a mortarium used for? Organic residues and cultural change in Iron Age and Roman Britain. *Antiquity*. 2011; 85: 1339–1352.
20. Cramp LJE, et al. Neolithic dairy farming at the extreme of agriculture in Northern Europe. *Proc Royal Soc B*. 2014; 281 20140819
21. Cramp LJE, et al. Immediate replacement of fishing with dairying by the earliest farmers of the northeast Atlantic archipelagos. *Proc Royal Soc B*. 2014; 281 20132372
22. Cramp LJE, et al. Regional diversity in subsistence among early farmers in Southeast Europe revealed by archaeological organic residues. *Proc Royal Soc B*. 2019; 286 20182347
23. Cramp LJE, Król D, Rutter M, Heyd VM, Pospieszny L. Analiza pozostałości organicznych z ceramiki kultury rzucewskiej z Rzucewa. *Pomorania Antiqua*. 2019; XXVIII: 245–259.
24. Cubas M, et al. Latitudinal gradient in dairy production with the introduction of farming in Atlantic Europe. *Nat Commun*. 2020; 11: 1–9. [PubMed: 31911652]
25. Debono Spiteri C, et al. Regional asynchronicity in dairy production and processing in early farming communities of the northern Mediterranean. *Proc Natl Acad Sci USA*. 2016; 113: 13594–13599. [PubMed: 27849595]
26. Demirci Ö, Lucquin A, Craig OE, Raemaekers DCM. First lipid residue analysis of Early Neolithic pottery from Swifterbant (the Netherlands, ca. 4300–4000 BC). *Archaeol Anthropol Sci*. 2020; 12: 105.
27. Demirci Ö, Lucquin A, Cakirlar C, Craig OE, Raemaekers DCM. Lipid residue analysis on Swifterbant pottery (c. 5000–3800 cal BC) in the Lower Rhine-Meuse area (the Netherlands) and its implications for human-animal interactions in relation to the Neolithisation process. *J Archaeol Sci Rep*. 2021; 36 102812
28. Dreslerová D, et al. Seeking the meaning of a unique mountain site through a multidisciplinary approach. The Late La Tène site at Sklá ské Valley, Šumava Mountains, Czech Republic. *Quat Int*. 2020; 542: 88–108.
29. Drieu L, et al. Chemical evidence for the persistence of wine production and trade in Early Medieval Islamic Sicily. *Proc Natl Acad Sci USA*. 2021; 118 e2017983118 [PubMed: 33619175]
30. Drieu L, et al. A Neolithic without dairy? Chemical evidence from the content of ceramics from the Pendimoun rock-shelter (Castellar, France, 5750–5150 BCE). *J Archaeol Sci Rep*. 2021; 35 102682
31. Dunne J, et al. Milk of ruminants in ceramic baby bottles from prehistoric child graves. *Nature*. 2019; 574: 246–248. [PubMed: 31554964]
32. Dunne J, Chapman A, Blinkhorn P, Evershed RP. Reconciling organic residue analysis, faunal, archaeobotanical and historical records: Diet and the medieval peasant at West Cotton, Raunds, Northamptonshire. *J Archaeol Sci*. 2019; 107: 58–70.
33. Dunne J, Chapman A, Blinkhorn P, Evershed RP. Fit for purpose? Organic residue analysis and vessel specialisation: The perfectly utilitarian medieval pottery assemblage from West Cotton, Raunds. *J Archaeol Sci*. 2020; 120 105178

34. Dunne J, et al. Finding Oxford's medieval Jewry using organic residue analysis, faunal records and historical documents. *Archaeol Anthropol Sci.* 2021; 13: 48.
35. Ethier J, et al. Earliest expansion of animal husbandry beyond the Mediterranean zone in the sixth millennium BC. *Sci Rep.* 2017; 7 7146 [PubMed: 28769118]
36. Evershed RP, Copley MS, Dickson L, Hansel FA. Experimental evidence for the processing of marine animal products and other commodities containing polyunsaturated fatty acids in pottery vessels. *Archaeometry.* 2008; 50: 101–113.
37. Fanti L, et al. The role of pottery in Middle Neolithic societies of western Mediterranean (Sardinia, Italy, 4500-4000 cal BC) revealed through an integrated morphometric, use-wear, biomolecular and isotopic approach. *J Archaeol Sci.* 2018; 93: 110–128.
38. Francés-Negro M, et al. Neolithic to Bronze Age economy and animal management revealed using analyses of lipid residues of pottery vessels and faunal remains at El Portalón de Cueva Mayor (Sierra de Atapuerca, Spain). *J Archaeol Sci.* 2021; 131 105380
39. Gregg MW, Banning EB, Gibbs K, Slater GF. Subsistence practices and pottery use in Neolithic Jordan: molecular and isotopic evidence. *J Archaeol Sci.* 2009; 36: 937–946.
40. Gunnarsson A, Oras E, Talbot HM, Ilves K, Legzdina D. Cooking for the living and the dead: lipid analyses of Rauši settlement and cemetery pottery from the 11th-13th century. *Estonian J Archaeol.* 2020; 24
41. Heron C, et al. Cooking fish and drinking milk? Patterns in pottery use in the southeastern Baltic, 3300-2400 cal BC. *J Archaeol Sci.* 2015; 63: 33–43.
42. Hoekman-Sites HA, Giblin JJ. Prehistoric animal use on the Great Hungarian Plain: A synthesis of isotope and residue analyses from the Neolithic and Copper Age. *J Anthropol Archaeol.* 2012; 31: 515–527.
43. Isaksson S, Hallgren F. Lipid residue analyses of Early Neolithic funnel-beaker pottery from Skogsmossen, eastern Central Sweden, and the earliest evidence of dairying in Sweden. *J Archaeol Sci.* 2012; 39: 3600–3609.
44. Krueger M, Bajev O, Whelton HL, Evershed RP. The Neolithic in the Middle Morava Valley. 2019; 3: 61–76.
45. Manzano E, et al. An integrated multianalytical approach to the reconstruction of daily activities at the Bronze Age settlement in Peñalosa (Jaén, Spain). *Microchem J.* 2015; 122: 127–136.
46. Manzano E, et al. Molecular and isotopic analyses on prehistoric pottery from the Virués-Martínez cave (Granada, Spain). *J Archaeol Sci Rep.* 2019; 27 101929
47. Matlova V, et al. Defining pottery use and animal management at the Neolithic site of Bylany (Czech Republic). *J Archaeol Sci Rep.* 2017; 14: 262–274.
48. McClure SB, et al. Fatty acid specific $\delta^{13}\text{C}$ values reveal earliest Mediterranean cheese production 7,200 years ago. *PLoS One.* 2018; 13 e0202807 [PubMed: 30183735]
49. Mileto S, Kaiser E, Rassamakin Y, Whelton H, Evershed RP. Differing modes of animal exploitation in North-Pontic Eneolithic and Bronze Age Societies. *Sci Technol Archaeol Res.* 2017; 3: 112–125.
50. Mukherjee AJ, Berstan R, Copley MS, Gibson AM, Evershed RP. Compound-specific stable carbon isotopic detection of pig product processing in British Late Neolithic pottery. *Antiquity.* 2007; 83: 743–754.
51. Mukherjee AJ, Gibson AM, Evershed RP. Trends in pig product processing at British Neolithic Grooved Ware sites traced through organic residues in potsherds. *J Archaeol Sci.* 2008; 35: 2059–2073.
52. Ogrinc N, Budja M, Potocnik D, Žibrat Gašpari A, Mlekuž D. Lipids, pots and food processing at Hocevarica, Ljubljansko barje, Slovenia. *Doc Praehist.* 2014; XLI: 181–194.
53. Oras E, et al. The adoption of pottery by north-east European hunter-gatherers: Evidence from lipid residue analysis. *J Archaeol Sci.* 2017; 78: 112–119.
54. Oras E, et al. Social food here and hereafter: Multiproxy analysis of gender-specific food consumption in conversion period inhumation cemetery at Kukruse, NE-Estonia. *J Archaeol Sci.* 2018; 97: 90–101.
55. Outram AK, et al. The earliest horse harnessing and milking. *Science.* 2009; 323: 1332–1335. [PubMed: 19265018]

56. Outram AK, et al. Horses for the dead: funerary foodways in Bronze Age Kazakhstan. *Antiquity*. 2010; 85: 116–128.
57. Outram AK, et al. Patterns of pastoralism in later Bronze Age Kazakhstan: new evidence from faunal and lipid residue analyses. *J Archaeol Sci*. 2012; 39: 2424–2435.
58. Özbal H, et al. Neolitik Bati Anadolu ve Marmara yerle imleri çanak çömleklerinde organik kalinti analizleri. *Arkeometri Sonuçlari Toplantisi*. 2013; 28: 105–114.
59. Özbal H, et al. Yenikapi, A a ipinar, Badema aci ve Barcin Çömleklerindeorganik kalinti analizi. *Arkeometri Sonuçlari Toplantisi*. 2013; 29: 83–90.
60. Pääkkönen M, Bläuer A, Evershed RP, Asplund H. Reconstructing food procurement and processing in early Comb ware period through organic residues in early Comb and Jakarla ware pottery. *Fennosc Archaeol*. 2016; XXXIII: 57–75.
61. Pääkkönen M, Bläuer A, Olsen B, Evershed RP, Asplund H. Contrasting patterns of prehistoric human diet and subsistence in northernmost Europe. *Sci Rep*. 2018; 8 1148 [PubMed: 29348633]
62. Pääkkönen M, Holmqvist E, Bläuer A, Evershed RP, Asplund H. Diverse economic patterns in the North Baltic Sea region in the Late Neolithic and Early Metal periods. *Eur J Archaeol*. 2019; 23: 4–21.
63. Papakosta V, Oras E, Isaksson S. Early pottery use across the Baltic - A comparative lipid residue study on Ertebølle and Narva ceramics from coastal hunter-gatherer sites in southern Scandinavia, northern Germany and Estonia. *J Archaeol Sci Rep*. 2019; 24: 142–151.
64. Pennetta A, Fico D, Lucrezia Savino M, Larocca F, Egidio De Benedetto G. Characterization of Bronze age pottery from the Grotte di Pertosa-Auletta (Italy): Results from the first analysis of organic lipid residues. *J Archaeol Sci Rep*. 2020; 31 102308
65. Pili iauskas G, et al. The Corded Ware culture in the Eastern Baltic: New evidence on chronology, diet, beaker, bone and flint tool function. *J Archaeol Sci Rep*. 2018; 21: 538–552.
66. Pili iauskas G, et al. Fishers of the Corded Ware culture in the Eastern Baltic. *Acta Archaeol*. 2020; 91: 95–120.
67. Robinson G, et al. Furness's first farmers: evidence of Early Neolithic settlement and dairying in Cumbria. *Proc Prehist*. 2020. 1–34.
68. Robson HK, et al. Diet, cuisine and consumption practices of the first farmers in the southeastern Baltic. *Archaeol Anthropol Sci*. 2019.
69. Roffet-Salque, M, Evershed, RP. Kopydłowo, stanowisko 6 Osady neolityczne z pogranicza Kujaw i Wielkopolski. Marciniak, Arkadiusz; Sobkowiak-Tabaka, Iwona; Bartkowiak, Marta; Lisowski, Mikolaj, editors. Wydawnictwo Profil-Archeo; 2015. 133–142.
70. Roffet-Salque, M, Banecki, B, Evershed, RP. Megalityczny grobowiec kultury amfor kulistych z Kierzkowa Milcz cy wiadek kultu przodków z epoki kamienia / A Megalithic tomb of the Globular Amphora Culture from Kierzkowo in the Paluki region - a silent witness of ancestor worship from the Stone Age Biskupin Archaeological Works. Nowaczyk, S, Pospieszny, L, Sobkowiak-Tabaka, I, editors. Archaeological Museum in Biskupin; 2017. 251–266.
71. Roffet-Salque, M, , et al. Ludwinowo 7 - Neolithic settlement in Kuyavia Saved Archaeological Heritage 8. Pyzel, Joanna, editor. Profil-Archeo Publishing House and Archaeological Studio, University of Gdansk Publishing House; 2019. 301–316. 9
72. Salque M, et al. New insights into the early Neolithic economy and management of animals in Southern and Central Europe revealed using lipid residue analyses of pottery vessels. *Anthropozoologica*. 2012; 47: 45–61.
73. Salque M, et al. Earliest evidence for cheese making in the sixth millennium BC in northern Europe. *Nature*. 2013; 493: 522–525. [PubMed: 23235824]
74. Smyth J, Evershed RP. The molecules of meals: new insight into Neolithic foodways. *Proc R Ir Acad*. 2015; 115C: 1–20.
75. Smyth J, Evershed RP. Milking the megafauna: Using organic residue analysis to understand early farming practice. *Environ Archaeol*. 2016; 21: 214–229.
76. Šoberl, L. Pots for the afterlife: organic residue analysis of British Early Bronze Age pottery from funerary contexts. PhD thesis, University of Bristol; 2011.

77. Šoberl L, Žibrat Gašpari A, Budja M, Evershed RP. Early herding practices revealed through organic residue analysis of pottery from the early Neolithic rock shelter of Mala Triglavca, Slovenia. *Doc Praehist.* 2008; 253–260.
78. Šoberl L, et al. Neolithic and Eneolithic activities inferred from organic residue analysis of pottery from Mala Triglavca, Moverna vas and Ajdovska jama, Slovenia. *Doc Praehist.* 2014; XLI: 149–179.
79. Spangenberg JE, Jacomet S, Schibler J. Chemical analyses of organic residues in archaeological pottery from Arbon Bleiche 3, Switzerland - evidence for dairying in the late Neolithic. *J Archaeol Sci.* 2006; 33: 1–13.
80. Spangenberg JE, Matuschik I, Jacomet S, Schibler J. Direct evidence for the existence of dairying farms in prehistoric Central Europe (4th mil. BC). *Isotopes Environ Health Stud.* 2008; 44: 189–200. [PubMed: 18569190]
81. Spataro M, et al. Production and function of Neolithic black-painted pottery from Schela Cladovei (Iron Gates, Romania). *Archaeol Anthropol Sci.* 2019.
82. Steele VJ, Stern B. Red Lustrous Wheelmade ware: Analysis of organic residues in Late Bronze Age trade and storage vessels from the eastern Mediterranean. *J Archaeol Sci Rep.* 2017; 16: 641–657.
83. Stojanovski D, et al. Living off the land: Terrestrial-based diet and dairying in the farming communities of the Neolithic Balkans. *PLoS One.* 2020; 15 e0237608 [PubMed: 32817620]
84. Stojanovski D, et al. Anta 1 de Val da Laje - the first direct view at diet, dairying practice and socio-economic aspects of pottery use in the final Neolithic of central Portugal. *Quat Int.* 2020; 542: 1–8.
85. Tarifa-Mateo N, et al. New insights from Neolithic pottery analyses reveal subsistence practices and pottery use in early farmers from Cueva de El Toro (Malagá, Spain). *Archaeol Anthropol Sci.* 2019.
86. Weber J, Brozio JP, Müller J, Schwark L. Grave gifts manifest the ritual status of cattle in Neolithic societies of northern Germany. *J Archaeol Sci.* 2020; 117 105122
87. Whelton HL, Roffet-Salque M, Kotsakis K, Urem-Kotsou D, Evershed RP. Strong bias towards carcass product processing at Neolithic settlements in northern Greece revealed through absorbed lipid residues of archaeological pottery. *Quat Int.* 2018; 496: 127–139.
88. Evershed RP, Heron C, Goad LJ. Analysis of organic residues of archaeological origin by high-temperature gas chromatography and gas chromatography-mass spectrometry. *Analyst.* 1990; 115: 1339–1342.
89. Correa-Ascencio M, Evershed RP. High throughput screening of organic residues in archaeological potsherds using direct methanolic acid extraction. *Anal Methods.* 2014; 6: 1330–1340.
90. Dudd SN, Evershed RP. Direct demonstration of milk as an element of archaeological economies. *Science.* 1998; 282: 1478–1481. [PubMed: 9822376]
91. Evershed RP, et al. Earliest date for milk use in the Near East and southeastern Europe linked to cattle herding. *Nature.* 2008; 455: 528–531. [PubMed: 18690215]
92. Dunne J, et al. First dairying in green Saharan Africa in the fifth millennium BC. *Nature.* 2012; 486: 390–394. [PubMed: 22722200]
93. Reimer PJ, et al. IntCal13 and Marine13 radiocarbon age calibration curves 0-50,000 years cal BP. *Radiocarbon.* 2013; 55: 1869–1887.
94. Bronk Ramsey C. Bayesian analysis of radiocarbon dates. *Radiocarbon.* 2009; 51: 337–360.
95. Collins R. What makes UK Biobank special? *Lancet.* 2012; 379: 1173–1174. [PubMed: 22463865]
96. Allen NE, Sudlow C, Peakman T, Collins R. UK Biobank Data: Come and Get It. *Sci Transl Med.* 2014; 6 224ed224
97. Enattah NS, et al. Identification of a variant associated with adult-type hypolactasia. *Nat Genet.* 2002; 30: 233–237. [PubMed: 11788828]
98. Graffelman J. Exploring Diallelic Genetic Markers: The HardyWeinberg Package. *J Stat Softw.* 2015; 64: 1–23.

99. Rodriguez S, Gaunt TR, Day INM. Hardy-Weinberg equilibrium testing of biological ascertainment for Mendelian randomization studies. *Am J Epidemiol.* 2009; 169: 505–514. [PubMed: 19126586]
100. Karczewski KJ, et al. The mutational constraint spectrum quantified from variation in 141,456 humans. *Nature.* 2020; 581: 434–443. [PubMed: 32461654]
101. Mitchell, R, Hemani, G, Dudding, T, Paternoster, L. UK Biobank Genetic Data: MRC-IEU Quality Control. University of Bristol; 2019. Version 2
102. Brumpton B, et al. Avoiding dynastic, assortative mating, and population stratification biases in Mendelian randomization through within-family analyses. *Nat Commun.* 2020; 11 3519 [PubMed: 32665587]
103. Howe LJ, et al. Genetic evidence for assortative mating on alcohol consumption in the UK Biobank. *Nat Commun.* 2019; 10 5039 [PubMed: 31745073]
104. Agranat-Tamir L, et al. The Genomic History of the Bronze Age Southern Levant. *Cell.* 2020; 181: 1146–1157. e1111 [PubMed: 32470400]
105. Allentoft ME, et al. Population genomics of Bronze Age Eurasia. *Nature.* 2015; 522: 167–172. [PubMed: 26062507]
106. Antonio ML, et al. Ancient Rome: A genetic crossroads of Europe and the Mediterranean. *Science.* 2019; 366: 708–714. [PubMed: 31699931]
107. Brace S, et al. Ancient genomes indicate population replacement in Early Neolithic Britain. *Nat Ecol Evol.* 2019; 3: 765–771. [PubMed: 30988490]
108. Broushaki F, et al. Early Neolithic genomes from the eastern Fertile Crescent. *Science.* 2016; 353: 499–503. [PubMed: 27417496]
109. Brunel S, et al. Ancient genomes from present-day France unveil 7,000 years of its demographic history. *Proc Natl Acad Sci USA.* 2020; 117 12791 [PubMed: 32457149]
110. Cassidy LM, et al. Neolithic and Bronze Age migration to Ireland and establishment of the insular Atlantic genome. *Proc Natl Acad Sci USA.* 2015; 113: 368–373. [PubMed: 26712024]
111. Cassidy LM, et al. A dynastic elite in monumental Neolithic society. *Nature.* 2020; 582: 384–388. [PubMed: 32555485]
112. Damgaard, PdB; , et al. 137 ancient human genomes from across the Eurasian steppes. *Nature.* 2018; 557: 369–374. [PubMed: 29743675]
113. Damgaard, PdB; , et al. The first horse herders and the impact of early Bronze Age steppe expansions into Asia. *Science.* 2018; 360 eaar7711 [PubMed: 29743352]
114. Feldman M, et al. Ancient DNA sheds light on the genetic origins of early Iron Age Philistines. *Sci Adv.* 2019; 5 eaax0061 [PubMed: 31281897]
115. Fernandes DM, et al. The spread of steppe and Iranian-related ancestry in the islands of the western Mediterranean. *Nat Ecol Evol.* 2020; 4: 334–345. [PubMed: 32094539]
116. Fu Q, et al. The genetic history of Ice Age Europe. *Nature.* 2016; 534: 200–205. [PubMed: 27135931]
117. González-Fortes G, et al. Paleogenomic Evidence for Multi-generational Mixing between Neolithic Farmers and Mesolithic Hunter-Gatherers in the Lower Danube Basin. *Curr Biol.* 2017; 27: 1801–1810. e1810 [PubMed: 28552360]
118. González-Fortes G, et al. A western route of prehistoric human migration from Africa into the Iberian Peninsula. *Proc Royal Soc B.* 2019; 286 20182288
119. Günther T, et al. Population genomics of Mesolithic Scandinavia: Investigating early postglacial migration routes and high-latitude adaptation. *PLoS Biol.* 2018; 16
120. Haber M, et al. Continuity and Admixture in the Last Five Millennia of Levantine History from Ancient Canaanite and Present-Day Lebanese Genome Sequences. *Am J Hum Genet.* 2017; 101: 274–282. [PubMed: 28757201]
121. Harney E, et al. Ancient DNA from Chalcolithic Israel reveals the role of population mixture in cultural transformation. *Nat Commun.* 2018; 9 3336 [PubMed: 30127404]
122. Hofmanová Z, et al. Early farmers from across Europe directly descended from Neolithic Aegeans. *Proc Natl Acad Sci USA.* 2016; 113: 6886–6891. [PubMed: 27274049]

123. Järve M, et al. Shifts in the Genetic Landscape of the Western Eurasian Steppe Associated with the Beginning and End of the Scythian Dominance. *Curr Biol.* 2019; 29: 2430–2441. e2410 [PubMed: 31303491]
124. Jones ER, et al. The Neolithic Transition in the Baltic Was Not Driven by Admixture with Early European Farmers. *Curr Biol.* 2017; 27: 576–582. [PubMed: 28162894]
125. Keller A, et al. New insights into the Tyrolean Iceman’s origin and phenotype as inferred by whole-genome sequencing. *Nat Commun.* 2012; 3 698 [PubMed: 22426219]
126. Krzewi ska M, et al. Ancient genomes suggest the eastern Pontic-Caspian steppe as the source of western Iron Age nomads. *Sci Adv.* 2018; 4 eaat4457 [PubMed: 30417088]
127. Lamnidis TC, et al. Ancient Fennoscandian genomes reveal origin and spread of Siberian ancestry in Europe. *Nat Commun.* 2018; 9 5018 [PubMed: 30479341]
128. Lazaridis I, et al. Ancient human genomes suggest three ancestral populations for present-day Europeans. *Nature.* 2014; 513: 409–413. [PubMed: 25230663]
129. Lazaridis I, et al. Genomic insights into the origin of farming in the ancient Near East. *Nature.* 2016; 536: 419–424. [PubMed: 27459054]
130. Lazaridis I, et al. Genetic origins of the Minoans and Mycenaeans. *Nature.* 2017; 548: 214–218. [PubMed: 28783727]
131. Linderholm A, et al. Corded Ware cultural complexity uncovered using genomic and isotopic analysis from south-eastern Poland. *Sci Rep.* 2020; 10 6885 [PubMed: 32303690]
132. Lipson M, et al. Parallel palaeogenomic transects reveal complex genetic history of early European farmers. *Nature.* 2017; 551: 368–372. [PubMed: 29144465]
133. Malmström H, et al. The genomic ancestry of the Scandinavian Battle Axe Culture people and their relation to the broader Corded Ware horizon. *Proc Royal Soc B.* 2019; 286 20191528
134. Marcus JH, et al. Genetic history from the Middle Neolithic to present on the Mediterranean island of Sardinia. *Nat Commun.* 2020; 11 939 [PubMed: 32094358]
135. Margaryan A, et al. Population genomics of the Viking world. *Nature.* 2020; 585: 390–396. [PubMed: 32939067]
136. Martiniano R, et al. The population genomics of archaeological transition in west Iberia: Investigation of ancient substructure using imputation and haplotype-based methods. *PLoS Genet.* 2017; 13 e1006852 [PubMed: 28749934]
137. Mathieson I, et al. Genome-wide patterns of selection in 230 ancient Eurasians. *Nature.* 2015; 528: 499–503. [PubMed: 26595274]
138. Mathieson I, et al. The genomic history of southeastern Europe. *Nature.* 2018; 555: 197–203. [PubMed: 29466330]
139. Mittnik A, et al. Kinship-based social inequality in Bronze Age Europe. *Science.* 2019; 93 eaax6219
140. Narasimhan VM, et al. The formation of human populations in South and Central Asia. *Science.* 2019; 365
141. Olalde I, et al. A common genetic origin for early farmers from Mediterranean Cardial and Central European LBK cultures. *Mol Biol Evol.* 2015; 32: 3132–3142. [PubMed: 26337550]
142. Olalde I, et al. The Beaker phenomenon and the genomic transformation of northwest Europe. *Nature.* 2018; 555: 190–196. [PubMed: 29466337]
143. Olalde I, et al. The genomic history of the Iberian Peninsula over the past 8000 years. *Science.* 2019; 363: 1230–1234. [PubMed: 30872528]
144. Rivollat M, et al. Ancient genome-wide DNA from France highlights the complexity of interactions between Mesolithic hunter-gatherers and Neolithic farmers. *Sci Adv.* 2020; 6 eaaz5344 [PubMed: 32523989]
145. Saag L, et al. Extensive Farming in Estonia Started through a Sex-Biased Migration from the Steppe. *Curr Biol.* 2017; 27: 2185–2193. e2186 [PubMed: 28712569]
146. Sánchez-Quinto F, et al. Megalithic tombs in western and northern Neolithic Europe were linked to a kindred society. *Proc Natl Acad Sci USA.* 2019; 116: 9469–9474. [PubMed: 30988179]
147. Schuenemann VJ, et al. Ancient Egyptian mummy genomes suggest an increase of Sub-Saharan African ancestry in post-Roman periods. *Nat Commun.* 2017; 8 15694 [PubMed: 28556824]

148. Schroeder H, et al. Unraveling ancestry, kinship, and violence in a Late Neolithic mass grave. *Proc Natl Acad Sci USA*. 2019; 116: 10705–10710. [PubMed: 31061125]
149. Skoglund P, et al. Genomic diversity and admixture differs for Stone-Age Scandinavian foragers and farmers. *Science*. 2014; 344: 747–750. [PubMed: 24762536]
150. Skourtanioti E, et al. Genomic History of Neolithic to Bronze Age Anatolia, Northern Levant, and Southern Caucasus. *Cell*. 2020; 181: 1158–1175. e1128 [PubMed: 32470401]
151. Unterlander M, et al. Ancestry and demography and descendants of Iron Age nomads of the Eurasian Steppe. *Nat Commun*. 2017; 8 14615 [PubMed: 28256537]
152. Valdiosera C, et al. Four millennia of Iberian biomolecular prehistory illustrate the impact of prehistoric migrations at the far end of Eurasia. *Proc Natl Acad Sci USA*. 2018; 115: 3428–3433. [PubMed: 29531053]
153. Villalba-Mouco V, et al. Survival of Late Pleistocene Hunter-Gatherer Ancestry in the Iberian Peninsula. *Curr Biol*. 2019; 29: 1169–1177. e1167 [PubMed: 30880015]
154. Wang C-C, et al. Ancient human genome-wide data from a 3000-year interval in the Caucasus corresponds with eco-geographic regions. *Nat Commun*. 2019; 10 590 [PubMed: 30713341]
155. Reich D. Allen Ancient DNA Resource (AADR): Downloadable genotypes of present-day and ancient DNA data. 2021. V44.3. <https://reich.hms.harvard.edu/allen-ancient-dna-resource-aadr-downloadable-genotypes-present-day-and-ancient-dna-data>
156. Li H, et al. The Sequence Alignment/Map format and SAMtools. *Bioinformatics*. 2009; 25: 2078–2079. [PubMed: 19505943]
157. Felsenstein, J. Theoretical evolutionary genetics. University of Washington; Seattle: 2016.
158. Brest J, Greiner S, Boskovic B, Mernik M, Zumer V. Self-adapting control parameters in differential evolution: A comparative study on numerical benchmark problems. *IEEE Trans Evol Comput*. 2006; 10: 646–657.
159. R Core Team. R: A language and environment for statistical computing. R foundation for statistical computing; 2018. Available at <http://www.R-project.org/>
160. Revell LJ. learnPopGen: An R package for population genetic simulation and numerical analysis. *Ecol Evol*. 2019; 9: 7896–7902. [PubMed: 31380058]
161. Jewett EM, Steinrücken M, Song YS. The Effects of Population Size Histories on Estimates of Selection Coefficients from Time-Series Genetic Data. *Mol Biol Evol*. 2016; 33: 3002–3027. [PubMed: 27550904]
162. Weninger, B. CalPal-2007. Cologne radiocarbon calibration & palaeoclimate research package; 2007. <http://www.calpal.de>
163. Galate P. BANADORA, Banque de données des dates radiocarbone de Lyon pour l'Europe et le Proche-Orient. 2011. <http://www.archeometrie.mom.fr/banadora>
164. Hinz M, et al. RADON-Radiocarbon dates online 2012. Central European database of 14C dates for the Neolithic and the Early Bronze Age. *Journal of Neolithic Archaeology*. 2012.
165. Manning K, Colledge S, Crema ER, Shennan S, Timpson A. The Cultural Evolution of Neolithic Europe. EUROEVOL Dataset 1: Sites, Phases and Radiocarbon Data. *JOAD*. 2016; 5
166. Burrow, S, Williams, S. The Wales and Borders Radiocarbon Database. Amgueddfa Cymru; National Museum Wales: 2008.
167. Ralston I, Ashmore P. Canmore Scottish Radiocarbon Database. <https://canmore.org.uk/project/919374>
168. Balsera V, Díaz-dei-Riío P, Gilman A, Uriarte A, Vicent JM. Approaching the demography of late prehistoric Iberia through summed calibrated date probability distributions (7000-2000 cal BC). *Quat Int*. 2015; 386: 208–211.
169. Vermeersch PM. Radiocarbon Palaeolithic Europe Database v.18. 2015. <https://ees.kuleuven.be/geography/projects/14c-palaeolithic/index.html>
170. Manning K. The Cultural Evolution of Neolithic Europe. EUROEVOL Dataset 2: Zooarchaeological data. *JOAD*. 2016; 5
171. Manning K, et al. The origins and spread of stock-keeping: the role of cultural and environmental influences on early Neolithic animal exploitation in Europe. *Antiquity*. 2013; 87: 1046–1059.

172. Stackhouse, PW, , Jr, et al. POWER release 8 (with GIS applications) methodology (data parameters, sources, & validation) documentation date may 1, 2018 (all previous versions are obsolete)(data version 8.0. 1). NASA; 2018. Retrieved from <https://power.larc.nasa.gov>

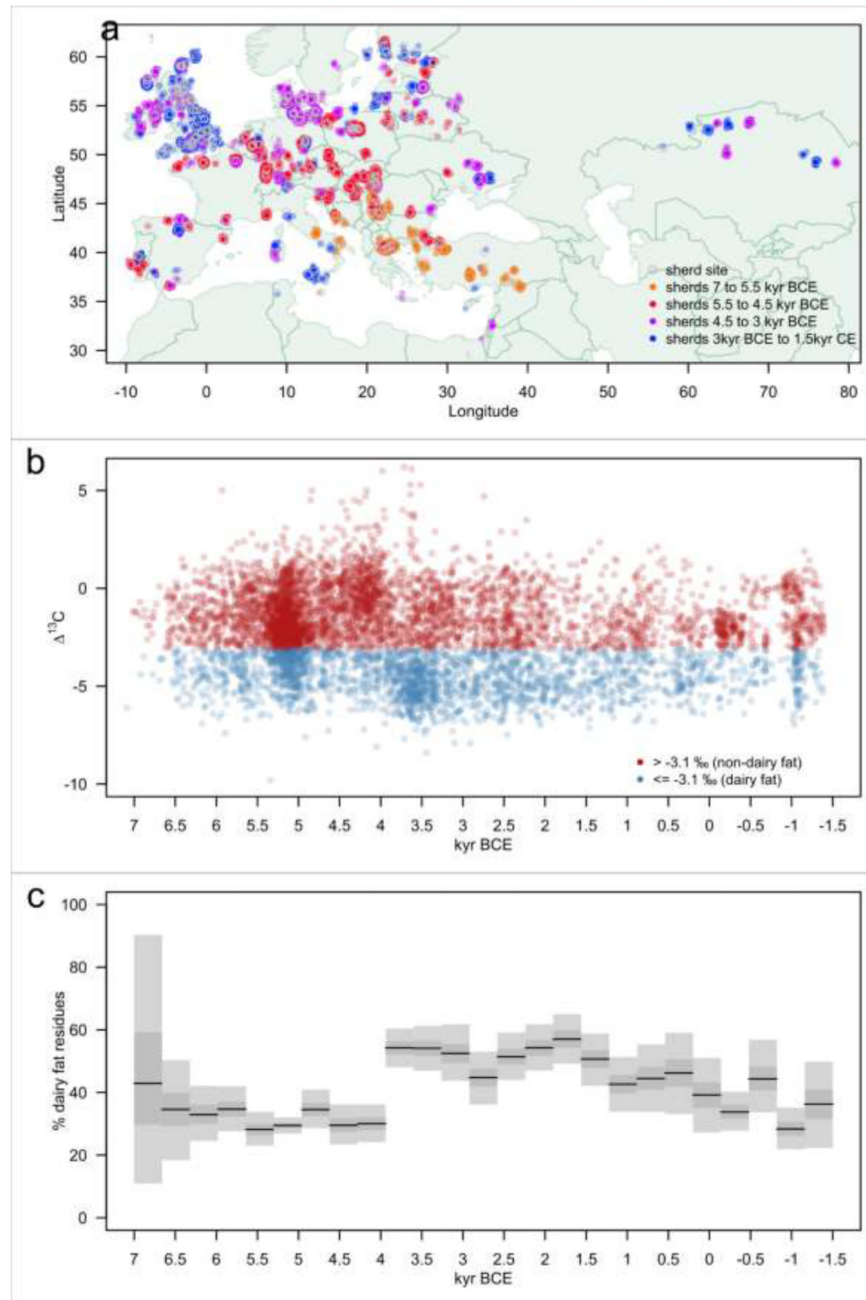


Figure 1. Geographic and temporal distribution of archaeological milk fat residues in potsherds. (a) Coloured circles illustrate 6,899 potsherds with animal fats from 826 phases from 554 sites (grey circles). Coloured circles are jittered to prevent perfect overlay, enabling the number of sherds to be visualised. (b) Plot of ^{13}C values for all 6,899 animal fat residues extracted from prehistoric potsherds through time. Each point corresponds to an individual measurement on a potsherd, with its position on the Y-axis randomly sampled from the uniform date range of the associated archaeological phase. Animal fats with ^{13}C values $> -3.1\text{‰}$ are defined as ruminant milk fats. Mare's milk is not characterised using this proxy⁸⁴

and would thus be defined as —non-milk”. (c) Percentage of dairy fat residues through time, calculated using all animal fat residues. Grey bars and black lines illustrate 95%, 50% Credible Intervals and Maximum a Posteriori in each time slice, using a uniform prior.

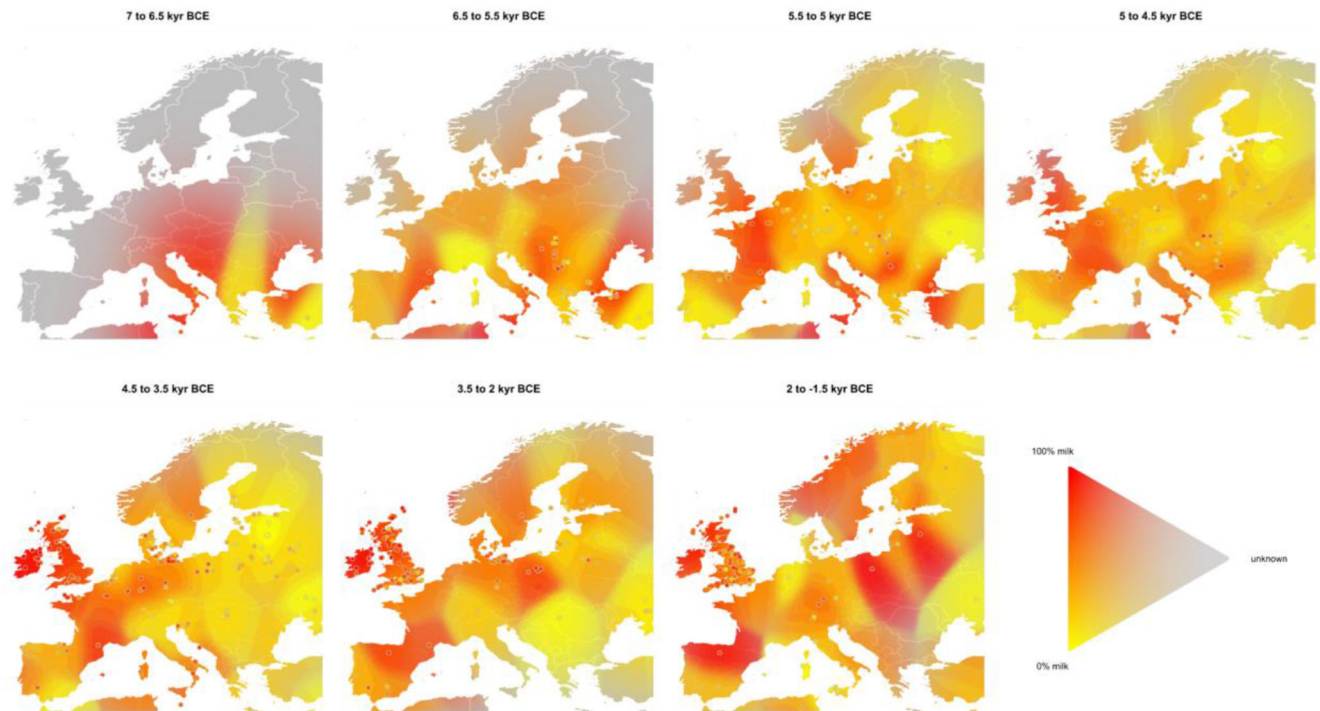


Figure 2. Regional variation in milk use in prehistoric Europe.

Interpolated time slices of the frequency of dairy fat residues in potsherds (colour hue) and confidence in the estimate (colour saturation) using 2D kernel density estimation. Bandwidth and saturation parameters were optimised using cross-validation. Circles indicate the observed frequencies at site-phase locations. The broad SE to NW cline of colour saturation at the beginning of the Neolithic illustrates a sampling bias towards earliest evidence of milk. Substantial heterogeneity in milk exploitation is evident across mainland Europe. In contrast, British Isles and Western France maintain a gradual decline across 7ka after first evidence of milk c. 5.5 ka BCE. Note that interpolation can colour some areas (particularly islands) where no data is present.

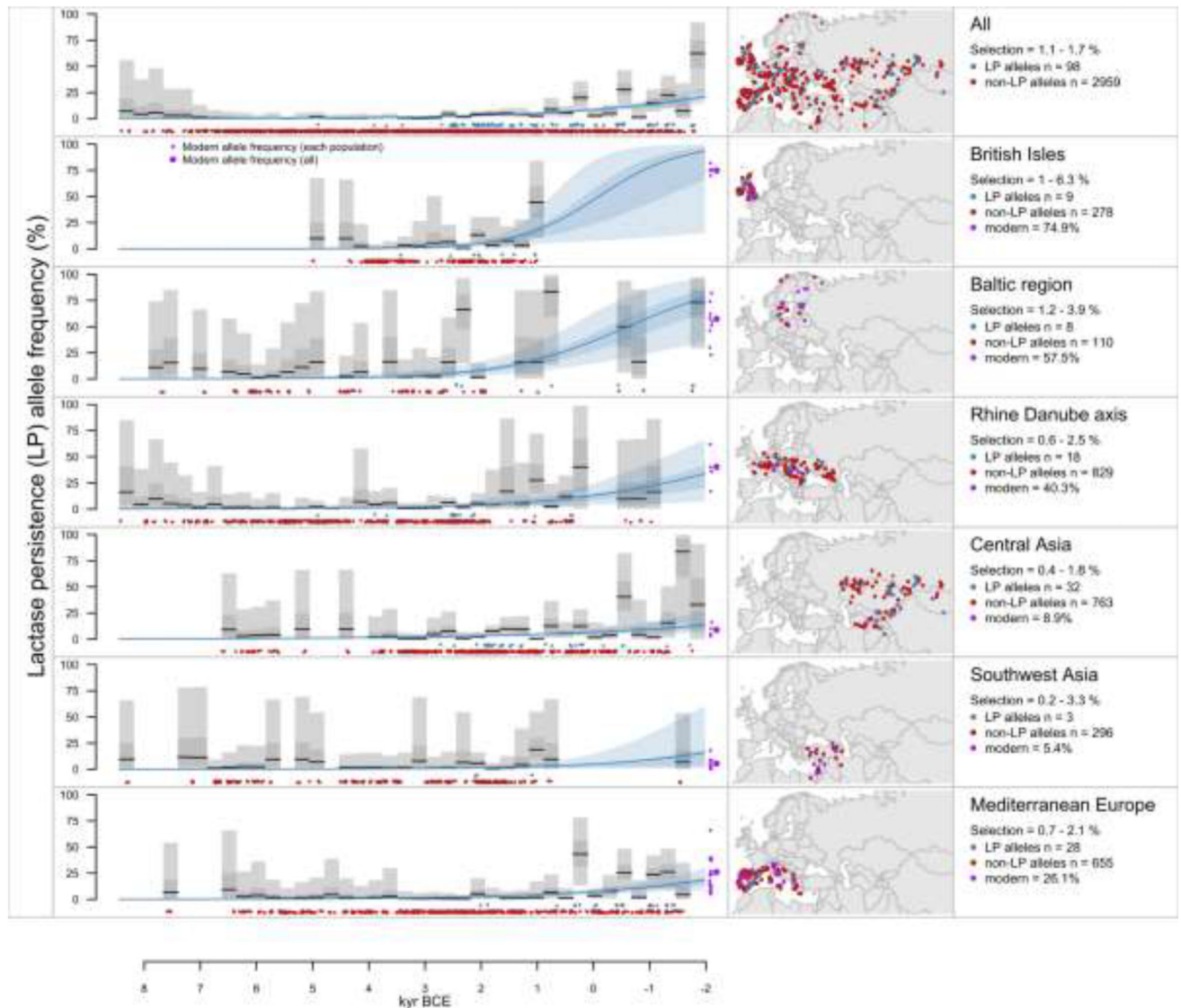


Figure 3. Regional variation in prehistoric LP allele frequencies in Europe.

Observed ancient DNA data illustrated with blue and red dots showing the date and location of 3,057 LP and LNP alleles (rs4988235-A and rs4988235-G, respectively) from 1,770 ancient individuals. Grey bars and black lines show the 95%, 50% Credible Intervals and Maximum a Posteriori in time slices, using a Jeffreys prior. Slices with no observations remain blank. Blue overlay illustrates the null model of a constant selection rate through time (different in each region), using the sigmoid curve (theoretical expectation). Blue lines illustrate maximum likelihood sigmoid curves fitted directly to the observed alleles. Blue shading represents the 95%, CI, 50% CI estimated from sigmoid joint parameters using MCMC. Likelihood function for sigmoid curves are constrained by three conservative prior beliefs to avoid absurd parameter combinations for regions with sparse data: 1) constant selection is below 10% per 28 yr generation; 2) LP frequencies are <1% at 10 kyr BCE; 3) LP frequencies are >1% at 2 kyr CE. Small purple dots represent observed LP frequencies

in modern populations in the same regions, as reported in Itan et al. supplementary data³², large purple dots represent a weighted average of these modern populations.

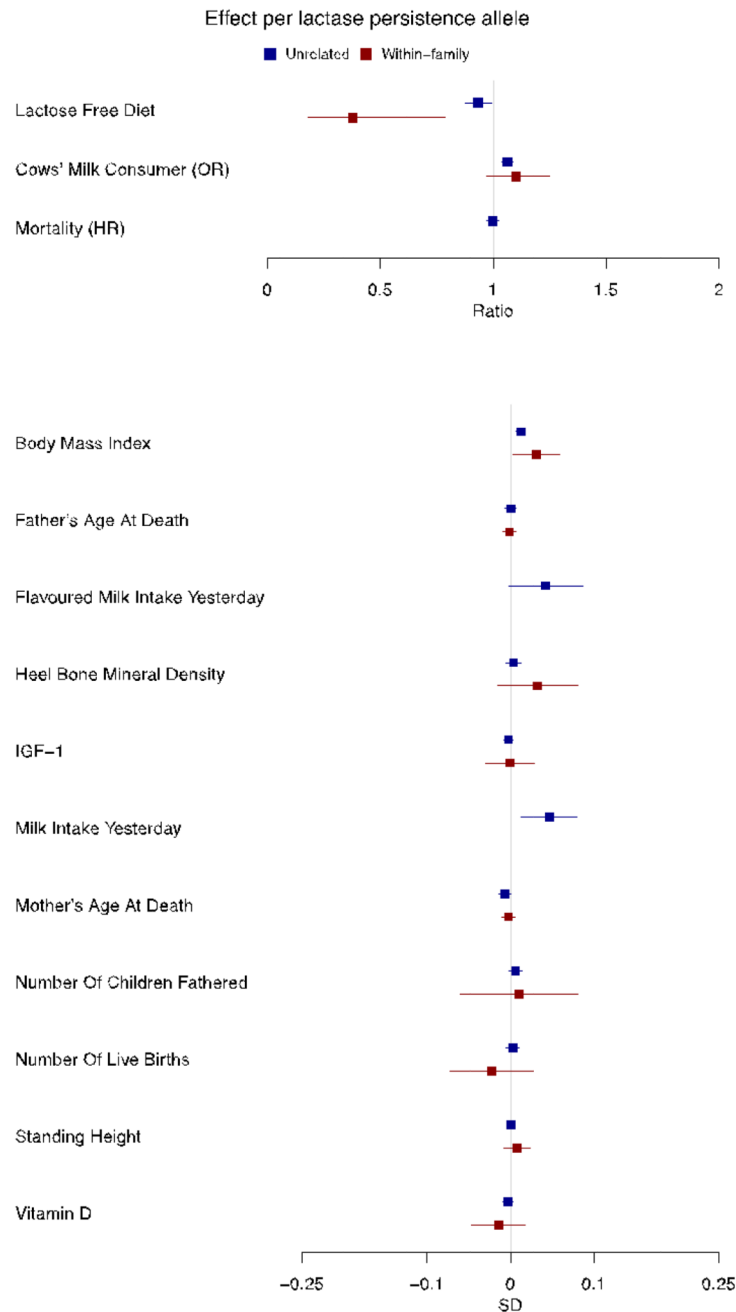
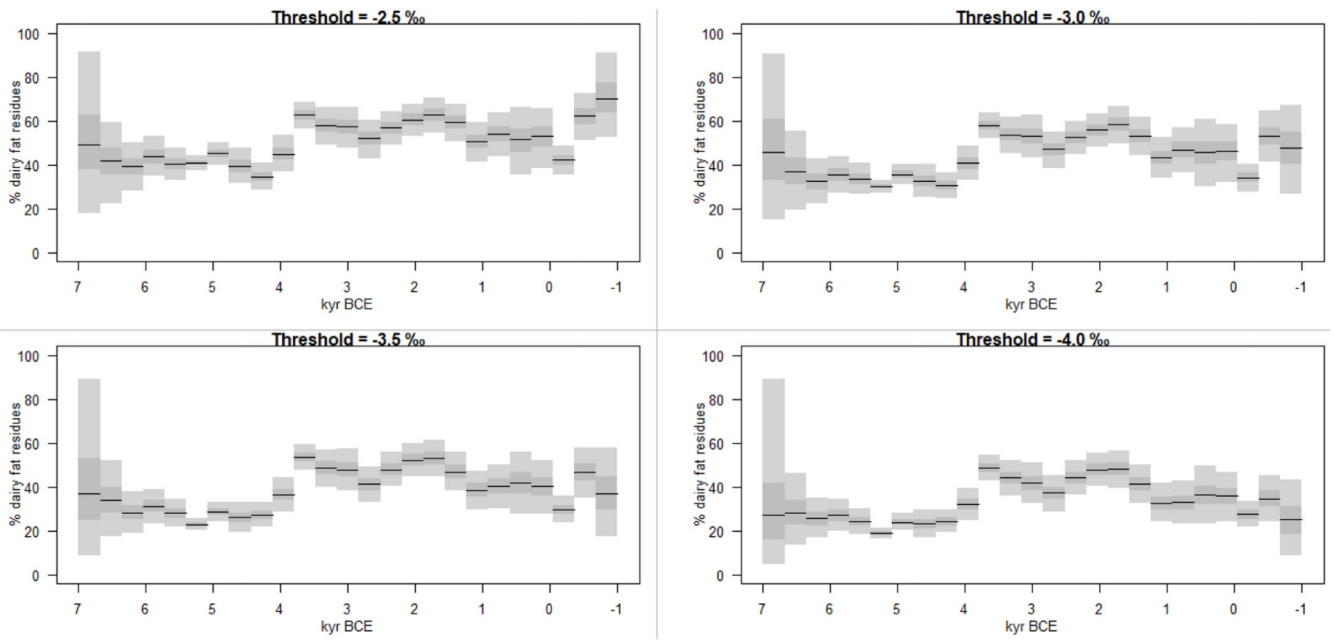


Figure 4. Lactase persistence variant association with health outcomes.

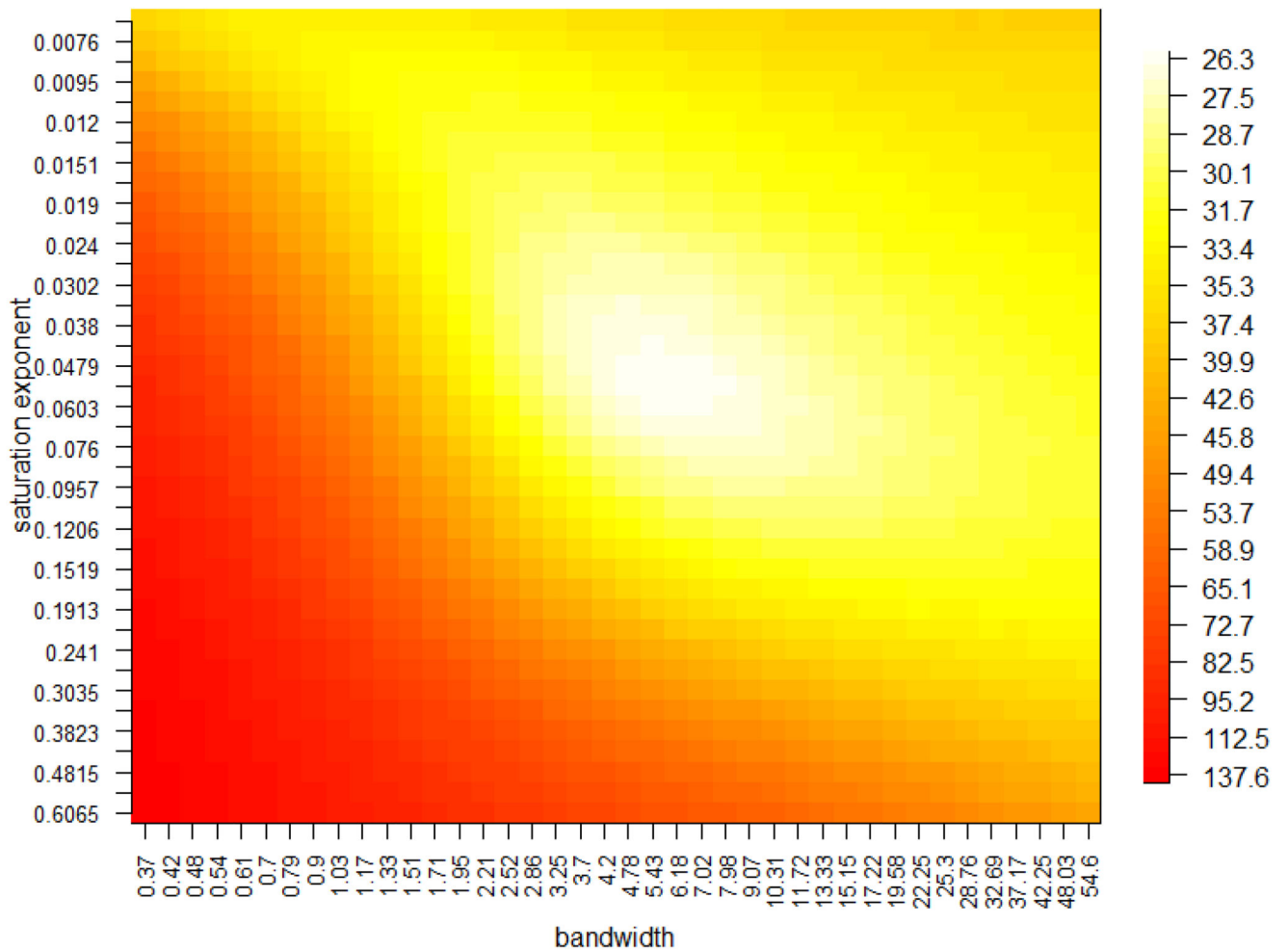
Variant associations with continuous (SD unit) or binary (OR/HR) outcomes adjusted for age, sex, and top 40 genetic principal components. Unrelated estimates were produced using an unrelated white British subset of UK Biobank ($n = 336,988$). Within-family estimates were produced using 40,273 siblings from 19,521 families. Within-family estimates of all cause-mortality, flavoured milk intake yesterday, and milk intake yesterday could not be determined. IGF-1, insulin-like -growth factor 1. OR, odds ratio. HR, hazard ratio. Lactose-free diet (derived from field 20086 from the UK Biobank); Cows' milk consumer (derived

from field 1418); Mortality (derived from field 40007); Body Mass Index (field 21001); Father's age at death (field 1807); Flavoured milk intake yesterday (field 100530); Heel bone mineral density (field 78); IGF-1 (field 30770); Milk intake yesterday (field 100520); Mother's age at death (field 3526); Number of children fathered (field 2405); Number of live births (field 2734); Standing height (field 50); Vitamin D (field 30890).



Methods Fig 1. Replication of Fig 1 tile C, using different thresholds for defining sherds as containing dairy fats. Correlation coefficients between all 6 comparisons vary from 0.712 to 0.982.

distance between accuracy and saturation



Methods Fig. 2. Bandwidth and saturation exponent parameters for interpolation plots were selected using a cross validation grid search, partitioning the observed data into an 80% training set and 20% test set. 1,000 random partitions were performed for each parameter pair, to generate a reliable summary statistic (distance between accuracy and saturation). Best estimates selected were bandwidth = 6.18 and the saturation exponent = 0.0538.

Table 1
Association of lactase persistence genotype and dairy milk intake.

Unadjusted genotype association with self-reported milk preference (non-dairy, i.e. soya and never/rarely have milk, vs dairy milk; derived from field 1418) in an unrelated white British subset of UK Biobank. The variant genotypes: GG, GA and AA at locus LCT -13910 produce non-lactase persistence (GG) and lactase persistence (GA/AA) phenotypes. Association P value was produced using the chi-square test.

Genotype	Non-milk drinkers		Milk drinkers		Total	P
GG – inferred LNP	1,646	8.1%	18,604	91.9%	20,250	
GA – inferred LP	8,374	6.8%	114,821	93.2%	123,195	
AA – inferred LP	12,672	6.7%	176,914	93.3%	189,586	
Total	22,692	6.8%	310,339	93.2%	333,031	8.5 x 10 ⁻¹⁴